The mechanosensitive ion channel PIEZO1 is expressed in tendons and regulates physical performance

Authors:

Ryo Nakamichi[1,2,3], Shang Ma[4], Takayuki Nonoyama[5], Tomoki Chiba[2], Ryota Kurimoto[2], Hiroki Ohzono[1], Merissa Olmer[1], Chisa Shukunami[6], Noriyuki Fuku[7], Guan Wang[8,9], Errol Morrison[10], Yannis P Pitsiladis[8,11], Toshifumi Ozaki[3], Darryl D'Lima[1], Martin Lotz[1], Ardem Patapoutian[4], and Hiroshi Asahara*[1,2]

Affiliations:

[1] Department of Molecular Medicine, Scripps Research, 10550 North Torrey Pines Road, MBB-102, La Jolla, California 92037, USA

[2] Department of Systems Biomedicine, Tokyo Medical and Dental University, 1-5-45 Yushima, Bunkyo-Ku, Tokyo 113-8510, Japan

[3] Department of Orthopaedic Surgery, Okayama University Graduate School of Medicine, Dentistry, and Pharmaceutical Sciences, Okayama 700-8558, Japan

[4] Howard Hughes Medical Institute, Department of Neuroscience, Dorris Neuroscience Center, Scripps Research, La Jolla, CA, 92037, USA

[5] Faculty of Advanced Life Science and Global Station for Soft Matter, Global Institution for Collaborative Research and Education (GSS, GI-CoRE), Hokkaido University, Sapporo, 001-0021, Japan

[6] Department of Molecular Biology and Biochemistry, Graduate School of Biomedical & Health Sciences, Hiroshima University, Hiroshima, 734-8553, Japan

[7] Graduate School of Health and Sports Science, Juntendo University, Chiba, 270-1965, Japan.

[8] School of Sport and Health Sciences, University of Brighton, Brighton, BN2 4AT, UK

[9] Centre for Regenerative Medicine and Devices, University of Brighton, Brighton, BN2 4AT, UK

[10] National Commission on Science and Technology, PCJ Building, 36 Trafalgar Road, Kingston 10, Jamaica

[11] Centre of Stress and Age-related Disease, University of Brighton, Brighton, BN2 4AT, UK

*Corresponding author: Email: asahara@scripps.edu

One Sentence Summary:

PIEZO1 acts as a critical mechanosensor in tenocytes, promoting tendon-specific gene expression, tendon function, and physical performance.

Abstract:

How mechanical stress affects physical performance via tendons is not fully understood. Piezo1 is a mechanosensitive ion channel, and E756 del *PIEZO1* was recently discovered as a gain-of-function variant that is common in individuals of African descent. We generated tendon-specific knock-in mice using R2482H *Piezo1*, a mouse gain-of-function variant, and found that they had higher jumping abilities and faster running speeds than wild-type or muscle-specific knock-in mice. These phenotypes were associated with enhanced tendon anabolism via an increase in tendon-specific transcription factors, Mohawk and Scleraxis, but there was no evidence of changes in muscle. Biomechanical analysis showed that the tendons of R2482H *Piezo1* mice were more compliant and stored more elastic energy, consistent with the enhancement of jumping ability. These phenotypes were replicated in mice with tendon-specific R2482H *Piezo1* replacement after tendon maturation, indicating that PIEZO1 could be a target for promoting physical performance by enhancing function in mature tendon. The frequency of E756 del *PIEZO1* was higher in sprinters than in population-matched non-athletic controls in a small Jamaican cohort, suggesting a similar function in humans. Taken together, this human and mouse genetic and physiological evidence revealed a critical function of tendons in physical performance, which is tightly and robustly regulated by PIEZO1 in tenocytes.

Main Text:

INTRODUCTION

The musculoskeletal system plays a central role in physical movement in animals. The kinetic energy required for physical movement is generated by the contraction of muscles, which is transmitted to the joints through tendons and ligaments. In this process, tendons may be perceived as solely passive connectors between the muscle and skeleton. However, studies have shown that the kangaroo genus performs a continuous hopping motion using the elastic energy of tendons in addition to the muscle energy (*1-3*). The mathematical relationship between the muscle-tendon complex and physical kinetic energy is described in Hill's model (*4*), in which physical kinetic energy is produced as the sum of the muscle's contracting power and the tendon's stored elastic energy power, indicating the critical function of the tendon to promote physical performance.

Mechanostimulation of the musculoskeletal system plays a major role in homeostasis of all tissues and organs (*5-7*). Appropriate mechanical stimulation of tendons is important for the maintenance of physical functions, since inactivity or immobilization of the human body leads to a reduction in tendon function, which causes musculoskeletal system disability (*8*). It is also known that appropriate physiological exercise load leads to an anabolic effect with increased tenogenic gene expression in humans (*9-11*). This anabolic effect of mechanical stimulation is expected to influence tendon function; however, little is known about the molecular mechanisms that sense mechanical stimuli in tendons and how this anabolic effect impacts physical performance.

In athletic performance research, it has been suggested that a certain degree of genetic predisposition is involved in the characteristics of athletic performance. For example, when examining athletic activities in international sports competitions, there are geographic regions that are strong in both instantaneous power and endurance sports events (*12, 13*). However, human

genetic polymorphisms that strongly correlate with instantaneous power have not yet been identified (*14-16*). PIEZO1 is a mechanically activated ion channel involved in mechanosensing in various organs and tissues (*17-20*), including bone (*21-23*) and cartilage (*24-26*). In humans, several single nucleotide polymorphisms (SNPs) in *PIEZO1* have been identified, some of which cause hereditary diseases (*27-30*). The E756 del gain-of-function variant is asymptomatic despite morphological changes in erythrocytes. However, it is protective against malaria (*31*), which explains its enrichment in regions with high rates of malaria, and it has also been linked to iron metabolism (*32*). This variant is present at an allele frequency of 16–18% in West African and African Americans and 3% in Europeans. We previously found that the mouse R2482H mutation of *Piezo1* provided resistance to malaria, similar to the human *PIEZO1* E756del variant, using systemic R2482H *Piezo1* mice (*Piezo1* $^{systemic\text{-}mut/+}$ mouse) (*31*). In this regard, Passini et al recently reported that the tendon property of *Piezo1* $^{systemic\text{-}mut/+}$ mouse was strengthened and humans carrying the PIEZO1 E756del gain-of-function variant show upregulated jumping ability, suggesting the potential link between PIEZO1 in tendon and motor function (*33*). However, whether and how PIEZO1 function in tendon could affect physical performance remains still unclear.

Here, taking advantage of this R2482H knock-in *Piezo1* mouse model, we elucidated the effect of the variant form of PIEZO1 in tendon-mediated physical performance, which is corroborated by human genetic studies. Furthermore, post-developmental replacement of the gain-of-function type of PIEZO1 in tenocytes also markedly promotes tendon properties and subsequent physical performance, suggesting that PIEZO1 in tendons could be a beneficial therapeutic target for musculoskeletal disorders and to improve human health.

RESULTS

Tendon-specific R2482H *Piezo1* mice have increased jumping power

To investigate the potential role of PIEZO1 activation in exercise capacity, we performed an established long jump test with 12-week-old wild type (*Piezo1* $^{cx/+}$) and systemic gain-of-function R2482H *Piezo1* (*Piezo1* $^{systemic\text{-}mut/+}$) mice (**fig. S1A**). This test involved placing a platform 80 cm above the ground and sequentially extending the distance between the platform and a cage at the same height, recording the maximum distance each mouse was able to jump back to the cage (*34*) (**fig. S1B**). The *Piezo1* $^{systemic\text{-}mut/+}$ mice (*Piezo1* $^{s\text{-}mut/+}$) could jump significantly farther than WT mice of both sexes (about 1.4-fold farther in males and 1.6-fold in females, **Fig. 1A, B, movie S1**). Next, to determine whether this enhanced jumping phenotype was derived from *Piezo1* acting primarily in the muscle or tendon, we created muscle-specific and tendon-specific R2482H *Piezo1* mice [*Piezo1* $^{muscle\text{-}mut/+}$ (*Piezo1* $^{m\text{-}mut/+}$) and *Piezo1* $^{tendon\text{-}mut/+}$ (*Piezo1* $^{t\text{-}mut/+}$), respectively] by crossing *Piezo1* $^{cx/+}$ mice with Myf5-Cre or Scx-Cre mice, respectively (**fig. S1A**). Similar to the *Piezo1* $^{systemic\text{-}mut/+}$ mice, the jumping distance of *Piezo1* $^{tendon\text{-}mut/+}$ mice increased significantly compared to WT mice in both sexes (about 1.4-fold in males and 1.7-fold in females, **Fig. 1A, B, movie S1**). In contrast, there was no increase in jumping distance of *Piezo1* $^{muscle\text{-}mut/+}$ mice compared to WT mice (**Fig. 1A, B, movie S1**).

Since the long jump test assesses instantaneous force generation, we also performed a run-to-exhaustion test to measure the effect of the *Piezo1* R2482H mutation on endurance (*35*) (**fig. S1C**). There was no difference in the running distance between the four groups (**Fig. 1C**). However, the maximum speed, which is an additional measure of instantaneous force, was again significantly higher in *Piezo1* $^{systemic\text{-}mut/+}$ mice and *Piezo1* $^{tendon\text{-}mut/+}$ mice than in WT mice and *Piezo1* $^{muscle\text{-}mut/+}$

mice of both sexes (**Fig. 1D**). These results suggest that PIEZO1 activation, specifically in tendon tissues, leads to stronger instantaneous power and increased speed but not endurance.

PIEZO1 is a mechano-sensitive ion channel in tenocytes

Following the results of the above physical performance tests, we analyzed the expression of *Piezo1* in specific cell types in muscular-tendon tissues by performing single-cell RNA sequencing (scRNA-seq) analysis of the Achilles tendon and hamstrings of 2-week-old mice. We found a relatively high expression of *Piezo1* in cells with high expression of *Mkx* and *Scx*, two major tendon-specific master transcription factors that regulate a set of tenogenic genes, including *Col1a1* and *Tnmd* (**Fig. 2A**) (*36-39*). In contrast, the expression of *Piezo1* was relatively low in cells with high *Myod1* expression (**Fig. 2A**). We also examined whether PIEZO1 functions as a calcium ion mechanoreceptor in tenocytes. Tenocytes were obtained from the Achilles tendon tissues of mice and patellar tendon tissue from young normal human donors during autopsy. Ca^{2+} influx into tenocytes via PIEZO1 was monitored using a Ca indicator in the presence or absence of Yoda1, a PIEZO1 agonist that increases the sensitivity of PIEZO1 (*40*). We found that Yoda1 increased Ca influx in a dose-dependent manner (**Fig. 2B**, **fig. S2**). Furthermore, Ca influx in the presence of Yoda1 in tenocytes of *Piezo1* $^{tendon\text{-}mut/+}$ mice was significantly higher than that in the tenocytes of WT mice (**Fig. 2C**). These results suggest that PIEZO1 acts as a calcium ion mechanoreceptor in tenocytes.

Strengthened tendon properties in R2482H *Piezo1* mice

To identify the physiological mechanisms involved in the R2482H *Piezo1*-mediated enhancement of instantaneous power in tenocytes, we performed a detailed morphological examination of

147 *Piezo1* $^{tendon\text{-}mut/+}$ mice compared with WT mice. We found a significantly wider Achilles tendon
148 in *Piezo1* $^{systemic\text{-}mut/+}$ and *Piezo1* $^{tendon\text{-}mut/+}$ mice than in WT mice and *Piezo1* $^{muscle\text{-}mut/+}$ mice (about
149 1.2-fold wider in both male and female *Piezo1* $^{tendon\text{-}mut/+}$ mice). This was not associated with
150 differences in the length of the Achilles tendon, body length, or body weight (**Fig. 3A, B, fig. S3A,**
151 **to C**). Furthermore, transmission electron microscopy (TEM) revealed a significantly larger
152 diameter of the cross-section of collagen fibrils of the Achilles tendon of *Piezo1* $^{systemic\text{-}mut/+}$ mice
153 and *Piezo1* $^{tendon\text{-}mut/+}$ mice than in WT mice (about 1.3-fold larger in male *Piezo1* $^{tendon\text{-}mut/+}$ mice
154 and 1.2-fold larger in female *Piezo1* $^{tendon\text{-}mut/+}$ mice). (**Fig. 3C to E, fig. S3D to F**). These results
155 suggested that R2482H *Piezo1* enhances tendon tissue formation and promotes tendon
156 enlargement.
157
158 **R2482H *Piezo1* in tenocytes enhances tenocyte-specific gene expression**
159 To identify the potential molecular mechanisms downstream of R2482H *Piezo1*, we analyzed the
160 gene expression profiles in the Achilles tendon of WT and *Piezo1* $^{tendon\text{-}mut/+}$ mice. RNA-Seq
161 analysis showed a significant upregulation of tendon-related genes, including *Scx* and *Mkx*, in
162 *Piezo1* $^{tendon\text{-}mut/+}$ mice (**Fig. 3F**). In contrast, the expression of muscle-related genes, including
163 *Myh7*, was downregulated in *Piezo1* $^{tendon\text{-}mut/+}$ mice compared to that in WT mice (**Fig. 3F**). In the
164 gene ontology enrichment analysis, "extracellular structure organization" and “skeletal system
165 development” were positively enriched terms with -log10(P) > 20, whereas "muscle structure
166 development" and “muscle system process” were negatively enriched terms with -log10(P) > 20
167 in the *Piezo1* $^{tendon\text{-}mut/+}$ mice (**Fig. 3G**). Focusing on the tendon components in the RNA-seq data,
168 the expression of multiple collagen and non-collagen matrices were shown to be upregulated (**table**
169 **S1**). Quantitative polymerase chain reaction (qPCR) analysis of Achilles tendons further verified

the upregulated expression of the above set of tendon-related genes, including *Mkx* and *Scx,* in *Piezo1* $^{systemic\text{-}mut/+}$ and *Piezo1* $^{tendon\text{-}mut/+}$ mice compared to WT and *Piezo1* $^{muscle\text{-}mut/+}$ mice (**Fig. 3H**). Based on these results, we further analyzed the Achilles tendon of WT and *Piezo1* $^{tendon\text{-}mut/+}$ mice. Picrosirius red staining showed that both tendons were yellow to red in color, which indicates that almost all fibers are type I collagen fibers, but the yellow coloration was stronger in *Piezo1* $^{tendon\text{-}mut/+}$ mice than in WT mice (**fig. S4A, B**). This indicated that the collagen density of *Piezo1* $^{tendon\text{-}mut/+}$ mice was lower than that of WT mice, suggesting the possibility of an increase in the non-collagen matrix in the interstices (*41, 42*). Therefore, we performed immunofluorescence staining of MKX, SCX, COL1A1, decorin (DCN), and proteoglycan 4 (PRG4) in tendons from WT and *Piezo1* $^{tendon\text{-}mut/+}$ mice. MKX- and SCX-positive cells were markedly increased in the tenocytes of *Piezo1* $^{tendon\text{-}mut/+}$ mice (**fig. S4C, D**). Both collagen and non-collagen matrices were more fluorescent in *Piezo1* $^{tendon\text{-}mut/+}$ mice, suggesting that these were more highly expressed (**fig. S4E, F**). Finally, to investigate the cellularity of the tendon, we performed immunostaining with an anti-Ki67 antibody for proliferation and completed TUNEL staining for apoptosis with Hoechst 33342; there was no observable difference between the two genotypes (**fig. S5**). These findings show that the expression of both collagen matrix- and non-collagen matrix-associated genes are enhanced in tenocytes with R2482H *Piezo1*, and this likely contributes to structural changes in the Achilles tendon of *Piezo1* $^{systemic\text{-}mut/+}$ mice and *Piezo1* $^{tendon\text{-}mut/+}$ mice.

PIEZO1 regulates *MKX* and *SCX* expression via NFATCs

Analysis of R2482H *Piezo1* mice revealed that PIEZO1 gain-of-function induces the expression of multiple tendon-related genes that alter tendon structure. MKX and SCX, tendon master regulators, are known to regulate gene expression of multiple tendon components (*36-39, 43-45*),

and our analysis suggests that PIEZO1 may regulate the expression of these transcription factors. To further investigate the mechanism of gene expression regulation through PIEZO1 activation, we first tested whether the activation of PIEZO1 affects the expression of *MKX* and *SCX* in human tenocytes. The expression of *MKX* and *SCX* was upregulated after mechanical stimulation with Yoda1 (**fig. S6A**). Next, we focused on calcineurin, which has been reported to be activated by PIEZO1 in osteoblasts (*23*). Calcineurin inhibition by cyclosporin A canceled the upregulation of these transcription factors by mechanical stimulation under Yoda1 administration, suggesting that calcineurin activation is important for the expression of these transcription factors (**fig. S6B**). Since NFATC 1, 2, 3, and 4 transcription factors are known to be transferred into the nucleus by calcineurin activation (*46, 47*), we examined the localization of these transcription factors after Yoda1 administration. The nuclear signal intensity of NFATC1, 2, and 4, but not NFATC3, increased upon stimulation with Yoda1 (**fig. S6C**). Finally, we performed knockdown experiments on NFATCs using siRNAs. Several groups of single NFATC knockdowns showed decreased expression of *MKX* and *SCX*, and mechanical stimulation under Yoda1 administration did not increase the expression of *MKX* in any group. Knockdown of NFATC1 or 3 upon mechanical stimulation under Yoda1 administration increased *SCX*, expression as compared to the control group, while knockdown of siNFATC4 abrogated this increase, and knockdown of NFATC1-4 further strengthened this tendency (**fig. S6D**, **fig. S7**). These results suggest that PIEZO1 induces the nuclear translocation of multiple NFATCs through the activation of calcineurin via Ca^{2+} influx, which regulates *MKX* and *SCX* expression.

R2482H *Piezo1* has no effect on muscle and nerve morphology

The above data show that R2482H *Piezo1* causes structural changes as well as significant changes

in gene expression in tendons. However, the enhanced generation of instantaneous force in *Piezo1* $^{systemic\text{-}mut/+}$ mice and *Piezo1* $^{tendon\text{-}mut/+}$ mice also suggest a potential effect on muscles, which produce contractile force. Thus, we compared muscles in the four genotypes of male mice by measuring the wet muscle weight of the lower legs, performing H&E staining to measure the anatomical cross-sectional area of muscle fibers, measuring the physiological cross-sectional area, and immunohistochemistry to determine the subtypes of myosin heavy chains in the lower limb muscles. We detected no differences among the four genotypes in any of these assays (**Fig. 4A–F**). Furthermore, we assessed alpha motor neuron endings and Golgi tendon organs in WT and *Piezo1* $^{tendon\text{-}mut/+}$ mice by whole-mount immunohistochemistry using several marker genes (*48*) to investigate whether muscle output is affected by changes in innervation: Again, there was no significant morphological difference (**fig. S8**). Taken together, our results suggest that the gain-of-function R2482H *Piezo1* mutation has no effect on muscle and nerve morphology; thus, the enhanced physical phenotype is directly caused by morphological changes in tendons.

Altered biomechanical capacity of tendons in R2482H *Piezo1* mice

For a more detailed physiological evaluation focusing on jumping motion, we performed high-speed video analysis using 18-week-old WT mice and *Piezo1* $^{tendon\text{-}mut/+}$ mice. The kinetic energy and angle of incidence of the jumping motion influence jumping distance (*49-51*). We verified that jump speed and kinetic energy correlated strongly with jump distance and that there was a weak correlation with the angle of incidence (**fig. S9, A to C**). This suggests that *Piezo1* $^{tendon\text{-}mut/+}$ mice increased their jumping distance by generating more energy during jumping motion mainly. Second, we traced the centroid position to evaluate the change in potential energy during the preparation phase and found that the centroid started shifting from a higher position in *Piezo1* $^{tendon\text{-}}$

$^{mut/+}$ mice, resulting in an about 2.3-fold increase in the potential energy variation compared to WT mice (**Fig. 5A–D**). Third, we focused on ankle joint motion during the jumping motion (*52*) and found that the ankle angle at maximum flexion in *Piezo1* $^{tendon\text{-}mut/+}$ mice was smaller than that in WT mice (**Fig. 5E–H**). These results of the video analysis suggest that *Piezo1* $^{tendon\text{-}mut/+}$ mice bend the ankle joint deeply using more potential energy changes. Next, we performed ex vivo static testing of the Achilles tendon to investigate its physical properties. The maximum stress and Young's modulus were decreased, although the toughness was not different in the Achilles tendon of *Piezo1* $^{tendon\text{-}mut/+}$ mice, apparently because of the enlarged cross-sectional area (**Fig. 5I, J, fig. S9D**). Furthermore, the elastic limit was significantly greater in *Piezo1* $^{tendon\text{-}mut/+}$ mice **(Fig. 5J)**. Although there was no difference in maximum load and stiffness, work to reach maximum load was significantly increased in *Piezo1* $^{tendon\text{-}mut/+}$ mice (**Fig. 5K, L, fig. S9E**). The results of high-speed video analysis and ex vivo static testing suggest that the R2482H *Piezo1* tendons are more compliant, which allows increased ankle flexion by increasing tendon extension.

Based on the above data, we predicted that *Piezo1* $^{tendon\text{-}mut/+}$ mice would store more elastic energy in the tendons during the preparation phase of jumping. We performed ex vivo tendon testing for each genotype to investigate the effect of PIEZO1 on energy production under conditions similar to the jumping movement. Tendons are known to stretch to a certain percentage of their elastic limit depending on the type of exercise, because they are damaged when stretched to their elastic limit (*53, 54*). In human tendon tests, the elastic limit of tendon elongation is about 8–10% (*55, 56*), and the stretch of the Achilles tendon during the preparation phase of a counter-movement jump is reported to be about 60% of the elastic limit (*57-59*). As it is currently difficult to directly measure tendon elongation during jumps in mice, the stored energy at 60% of the elastic limit for isolated tendons of each genotype (i.e., 60% of 16% = 9.5% for WT mice and 60% of

27% =16% for *Piezo1* $^{tendon\text{-}mut/+}$ mice) was analyzed. First, to evaluate the viscoelastic properties of the tendons, cyclic dynamic tests were performed in the range of 1–100 Hz at 60% of the strain at the average elastic limit of WT and *Piezo1* $^{tendon\text{-}mut/+}$ mice, respectively. Both WT and *Piezo1* $^{tendon\text{-}mut/+}$ mice showed a velocity-dependent increase in storage modulus, and conversely, a decrease in loss modulus and tan δ (**fig. S10**). However, the tan δ of both genotypes was very small at all frequencies, indicating that the viscous contribution was small in these tendons over the range of testing (**fig. S10**). Next, to calculate the energy stored in the Achilles tendon during the preparation phase, the velocity during the preparation phase of the Achilles tendon was calculated using the displacement conditions and preparation phase time obtained from high-speed video analysis (mean time of 0.0275 s for WT and 0.02542 s for *Piezo1* $^{tendon\text{-}mut/+}$ mice) and the dynamic test that represented the preparation phase for each genotype. The tendon-stored energy in *Piezo1* $^{tendon\text{-}mut/+}$ mice, calculated from the area under the unloading curve (**Fig. 5M**), was about 3-fold greater than that in WT mice (**Fig. 5N**). Additionally, the load on the Achilles tendon at maximum elongation in the *Piezo1* $^{tendon\text{-}mut/+}$ mice was about 1.7-fold greater than that in WT mice (**Fig. 5M**). Energy dissipation was also measured and was found to be lower in *Piezo1* $^{tendon\text{-}mut/+}$ mice (**Fig. 5O**). However, the percentage of energy dissipation to total energy content was small in both genotypes (4.7% on average for WT and 2.1% for *Piezo1* $^{tendon\text{-}mut/+}$ mice). Taken together, these results suggest that R2482H *Piezo1* mice use their increased tendon compliance to increase stored energy in the tendon.

R2482H *Piezo1* potentiates instantaneous physical performance postnatally

We next assessed whether the increased physical performance caused by the gain-of-function R2482H *Piezo1* mutation is due to effects on tendons that occur specifically during development

or whether the variant can also influence physical performance when introduced in the postnatal phase in mature animals. To test this, we generated conditional Scx-creERT2*: Piezo1*$^{cx/+}$ mice (=*Piezo1* $^{postnatal\text{-}tendon\text{-}mut/+}$ mice = *Piezo1* $^{p\text{-}t\text{-}mut/+}$ mice) to introduce the R2482H *Piezo1* variant postnatally (*60, 61*). Scx-CreERT2 (+) (WT) mice were used as the controls. Mice were treated with tamoxifen (100 mg/kg body weight, injected on five consecutive days) at 6 weeks of age (**fig. S11**). Our analysis of these *Piezo1* $^{postnatal\text{-}tendon\text{-}mut/+}$ mice showed increased Achilles tendon width macroscopically (**Fig. 6A, B**) and microscopically (**Fig. 6C-E**), and increased expression of tendon-related genes (**Fig. 6F**), despite less genetic recombination compared with *Piezo1* $^{tendon\text{-}mut/+}$ mice (**fig. S11**). The instantaneous physical ability of *Piezo1* $^{postnatal\text{-}tendon\text{-}mut/+}$ mice was also enhanced compared with that of WT mice (**Fig. 6G, H**). These findings suggest that R2482H *Piezo1* in tenocytes can potentiate tendon function and subsequent physical ability even after tendon maturation.

Elevated frequency of E756 del *PIEZO1* in Jamaican sprinters

The above findings that accelerated function of PIEZO1 in tendon could markedly promote the motor function in mice prompted us to examine the potential impact on the ability of human physical performance. Analysis of the ExAC database of approximately 60,000 exosomes showed that the *PIEZO1* E756 deletion, which is a mild gain-of-function variant compared to R2456H *PIEZO1* (the human equivalent of R2482H *Piezo1* in mice), was present in about 18% of individuals classified as “African-descent” in allele frequency (*31*). Individuals with E756 del acquire resistance to malaria and have altered iron metabolism (*31, 32*). However, the effects of the variant on motor function are not fully addressed yet. Given our results in R2482H *Piezo1* mice and the prior report that humans with E756 show upregulated jumping ability (*33*), we surveyed

the athletic ability of humans with *PIEZO1* E756 deletion. The Athlome consortium project aims to identify potential omics markers of athletic ability (*14*). Thus, we examined the frequency of the *PIEZO1* E756del ratio, selecting sprinters (who require substantial instantaneous force) and controls from Jamaica, where most of the population is of West African descent, to potentially enrich for the *PIEZO1* E756del mutant. Jamaican athletes who had participated in international competitions in sprinting, jumping, and throwing events (i.e., 100–400 m, jump, and throw) were defined as 'sprinters'. For comparison, Jamaican controls (students at the University of the West Indies) who had not competed in track events were analyzed (*15, 16*). Of the 91 Jamaican sprinters, 46% were heterozygous for the E756 del and 8% were homozygous. This was significantly different from the ethnicity-matched controls, where 31% of 108 individuals were heterozygous and 2% were homozygous **(Fig. 7A, Table 1)**. The frequency of the E756 del ratio was significantly increased in both sexes (**Fig. 7B, Table1**). These data lend preliminary support to the data obtained using the mouse model, suggesting that the E756 del may enhance natural athletic ability (i.e., instantaneous force), and support the importance of studying larger cohorts.

DISCUSSION

In this study, we revealed that a gain-of-function variant of PIEZO1 accelerates instantaneous power, such as jumping and running speed, through structural modification of the tendon tissue in mice. Furthermore, in a small human cohort study, we demonstrated that a relatively mild gain-of-function variant of PIEZO1, which is common in African Americans, Jamaicans, and West Africans, may be involved in sprinting ability. These results suggest that PIEZO1, a mechanically activated ion channel, plays an important role in tendon-mediated enhancement of instantaneous power.

Recently, Passini et al. (*33*) reported that PIEZO1 is a mechanosensor in tenocytes and that its activation in tenocytes accelerates Ca^{2+} influx by mechanostress, as well as in other cell types (*20-25, 31*). These findings are consistent with our observations. In addition, they also observed increased collagen crosslinks in tendons of systemic R2482H *Piezo1* mice and increased stiffness and maximum force biomechanically, compared to wild-type mice. However, there are no data on the potential effect of PIEZO1 gain-of-function on physical performance *in vivo*, even in systemic R2482H *Piezo1* mice. Here, we found that systemic R2482H *Piezo1* mice exhibited enhanced physical ability. Physical performance tests indicated that this *Piezo1* gain-of-function mutation specifically potentiated instantaneous power generation, such as jumping power and high-speed running. Furthermore, our study revealed that tendon-specific R2482H *Piezo1* mice, but not muscle-specific R2482H *Piezo1* mice, have enhanced physical performance comparable to systemic R2482H *Piezo1* mice, indicating a specific function of PIEZO1 in tenocytes. We demonstrated that enhanced physical performance could be acquired even after reaching skeletal maturity by introducing the tendon-specific replacement R2482H *Piezo1* by tamoxifen in 6-week-old mice.

Analysis of R2482H *Piezo1* mice revealed drastic transcriptome changes in tendons. *Scx* and *Mkx*, two transcription factors that play important roles in tendon formation, and their downstream genes *Tnmd*, *Col1a1*, and small leucine-rich proteins (SLRPs) such as *Dcn* and *Fmod*, were upregulated. Our study also showed that activation of PIEZO1 promotes the nuclear translocation of multiple NFATCs, which induces increased expression of MKX and SCX. Previous studies have shown that both *Scx*-and *Mkx*-knockout mice show hypoplastic tendons, and overexpression of these genes in stem cells increases tendon tissue synthesis (*36-39, 43-45*). Furthermore, these transcription factors are involved in tenocyte homeostasis in response to mechanical stress and in

the expression of their downstream genes, such as collagen and SLRPs (*62, 63*). Our study suggests that PIEZO1 plays a role in orchestrating mechanotransduction in tenocytes by regulating these two transcription factors through activation of NFTACs, and this mechanism is enhanced in R2482H *Piezo1* mice, thereby enhancing tendon synthesis. Furthermore, our histological analysis showed tendon tissue enlargement in male and female R2482H *Piezo1* mice, which was consistent with the results of our transcriptome analysis. Recently, Passini *et al.* (*33*) reported that morphological analysis of plantaris tendons from systemic R2482H *Piezo1* mice showed no expansion of collagen fibrils, whereas biomechanical analysis showed an increase in stiffness. Differences between our tendon-specific R2482H *Piezo1* mice and the systemic R2482H *Piezo1* mice used in (*33*) may reflect variations in mechanical loading in different tendon tissues or the plasticity of tendons affected by PIEZO1 throughout the body.

We did not detect any significant evidence of enhanced physical performance in muscle specific R2482H *Piezo1* mice. Additionally, muscle morphology was similar to WT mice, which suggests that PIEZO 1 is unlikely to directly affect muscle structure or function. We documented significant histological and structural changes in the tendons of systemic and tendon-specific R2482H *Piezo1* mice. It is possible that these changes in tendons can induce secondary changes in the muscle, such as muscle adaptation to increased tendon compliance. However, we found no evidence of alterations in muscle morphology to support the possibility of secondary adaptation in systemic and tendon-specific R2482H *Piezo1* mice.

Human sports medicine research has focused on the step motion observed during athletic activities, such as the countermovement jump. This step motion is called stretch-shortening cycle (SSC) motion (*64*) and can improve athletic performance (*65-67*). The mechanisms by which the SSC motion affects motor function can be divided into two broad categories. Some reports have

377 focused on muscle tissue, such as the effects of the SSC motion on the enhancement of muscle
378 contraction (*68-70*), whereas others have focused on tendon tissue in animals, such as the kangaroo,
379 which utilizes the stored energy in the tendon (*71-73*). Our study showed the possibility that stored
380 energy in tendons increased during jumping in tendon-specific R2482H *Piezo1* mice, but because
381 of the limitation that our experiment was based on elongation strain obtained from human Achilles
382 tendon data (57-59), it will be necessary to directly measure in vivo the individual contributions
383 of tendon and muscle shortening during jumping to more accurately calculate stored energy. The
384 increase in kinetic energy during jumping observed in our video analysis of the SSC motion
385 suggests the existence of a mechanism that enhances kinetic energy other than the increase in
386 stored energy in the tendons of R2482H *Piezo1* mice obtained in the dynamic test. Consistent with
387 our finding that accelerated tendon properties by R2482H *Piezo1* enhance jumping power,
388 previous reports have shown that changes in tendon properties affect maximal output from the
389 same muscle contraction stimulus (*74, 75*). It has been reported that non-collagen matrices may be
390 involved in tendon extensibility (*76, 77*). *Prg4-knockout* mice have increased tenon fascicle
391 gliding resistance compared to wild type mice (*78, 79*). Elastin is also postulated to contribute to
392 tendon elasticity (*80-82*). Furthermore, it has been shown that energy-storing tendons contain
393 more aggrecan (ACAN), biglycan (BGN), DCN, fibromodulin (FMOD) and cartilage oligomeric
394 matrix protein (COMP) than positional tendons (*83, 84*). In our study, the expression of several
395 non-collagen matrix components, such as PRG4 and DCN, was upregulated in the Achilles tendon
396 of tendon-specific R2482H *Piezo1* mice. These factors could be involved in tendon extensibility
397 and enhance output from muscle. It would be interesting to use this model to further study the
398 mechanism of muscle-tendon coordination.

399 This study also found that the frequency of E756 del *PIEZO1*, a human gain-of-function
400 variant, is increased in Jamaican sprinters. From a physiological perspective, studies have shown
401 that African Americans and West Africans have increased bone density (*85*) and lower body fat
402 content (*86*) but show no change in muscle structure (*87*). In recent years, efforts have been made
403 to elucidate differences in athletic performance originating genetically (*14*). The R577X
404 polymorphism in *ACTN3*, known as the performance gene, has been linked to muscle performance
405 and affects endurance by shifting muscle metabolism to more efficient aerobic pathways, which
406 conversely disadvantages instantaneous performance (*88-93*). Variants of *ACE* have also been
407 linked to performance. For example, I/D polymorphism is a 287-base pair (bp) Alu insertion in
408 intron 16 of the gene: The D allele is associated with power, and the I allele is associated with
409 endurance (*94-97*). These genes have also been investigated in Jamaican sprinters; however, no
410 correlation between polymorphisms in these genes and sprinting ability has been found (*15*).
411 Recently, we found that the *PIEZO1* gene polymorphism (E756 del) was present in 18% of the
412 African population, including African Americans and Jamaicans (*31*). Functional variants of
413 PIEZO1 have been reported as disease-causing genetic variants, such as loss-of-function mutations
414 that cause congenital lymphatic dysplasia (*30*) and gain-of-function mutations that cause
415 hereditary xerocytosis (*27, 29*). E756 del *PIEZO1* is a mild form of PIEZO1 gain-of-function
416 mutation associated with deformed erythrocytes and malaria resistance (*31*). In addition, although
417 iron overload in the blood occurs in old age, this is not observed in individuals younger than 40
418 years of age, who do not differ from those with wild-type PIEZO1(*31, 32*). Although our human
419 cohort study was small, the increased frequency of E756 del *PIEZO1* in sprinters indicates the
420 potential of this PIEZO1 variant to act as a performance gene. Consistent with our results, a small
421 clinical study reported that humans with this E756 del may have improved performance in jumping

movements that place high loads on tendons (*59*). The results of our and others' relatively small human genetics studies support the importance of future large-scale studies focusing on E756 del *PIEZO1* to elucidate the relationship between human physical performance and genetic background.

Lastly, strengthened physical ability could be acquired postnatally by conversion of wild-type *Piezo1* to R2482H *Piezo1* in tenocytes, which leads to an associated increase in tendon-related genes. This supports the potential of targeting PIEZO1 in tenocytes to improve physical performance when it is compromised in disease states. Tendinopathy is characterized by painful loss of motor function and is an important clinical problem in musculoskeletal and sports-related medicine (*98*). SCX and MKX, which are responsible for PIEZO1-mediated mechanotransduction in tenocytes, are also important factors in tendon growth after birth (*99, 100*). Similarly, these two transcription factors have been shown to correlate with cell damage and loss under conditions of low expression (*100, 101*). Therefore, regulation of SCX and MKX expression by targeting PIEZO1 has the potential to become a preventive medicine for tendon disorder-related diseases and to improve or maintain human physical performance. These findings may contribute to the development of novel preventive and therapeutic strategies for common musculoskeletal disorders, as well as deterioration during aging.

Although we found an unexpected function of the PIEZO1-mediated structural modification of tendons that improves physical function, unresolved questions remain. These include: the need for more accurate evaluation of the stored elastic energy in tendons during jumping; investigating the potential relationship between changes in tendon properties and muscle function; and confirming and extending the finding of an increased frequency of E756 del *PIEZO1* in sprinters

444 in a larger cohort study. Addressing these issues should lead to a more complete understanding of
445 the physiological and physical functions of tendons.

446 In summary, we found that PIEZO1 acts as a critical mechanosensor in tenocytes, promoting
447 tendon function by inducing tendon-specific gene expression and structural changes, resulting in
448 enhanced motor function. Tendons can markedly affect the processes of saving chemical energy
449 and converting and expressing it into kinetic energy, resulting in improvements in physical
450 performance. Understanding the PIEZO1-mediated mechanobiology of tendons could inform
451 future studies on potential applications for athletic performance and medical applications for
452 musculoskeletal disorders.
453

MATERIALS AND METHODS

Study design

The primary goal of this study was to determine whether *Piezo1* gain-of-function mutations affect motor function and to identify the tissues involved. We investigated multiple tissue-specific *Piezo1* gain-of-function mutant mice and found that tendons with *Piezo1* gain-of-function mutations affected motor function. Next, we performed biological and biomechanical analyses to determine the changes in tendons with *Piezo1* gain-of-function mutations and how these affected motor function. We also performed a small-scale human cohort study to assess associations between *PIEZO1* gain-of-function variant and human athletic ability. All animal experiments were performed with the approval of the Scripps Institutional Animal Care and Use Committee. Human tissues for the experiments using human patella tendon derived cells were obtained with the approval of the Scripps Human Subjects Committee. Motor function tests in mice were performed by two independent observers who were not privy to the experimental conditions.

Mice

All animal procedures were approved by the Institutional Animal Care and Use Committee of the Scripps Research Institute. *Piezo1* $^{systemic\text{-}mut/+}$ mice, *Piezo1* $^{tendon\text{-}mut/+}$ mice, *Piezo1* $^{postnatal\text{-}tendon\text{-}mut/+}$ mice, and *Piezo1* $^{muscle\text{-}mut/+}$ mice were generated by breeding *Piezo1*$^{cx/cx}$ mice with Cmv-Cre mice (Jackson Laboratory stock# 006054), Scx-Cre mice (a gift from Dr. Shukunami at Hiroshima University), Scx-CreERT2 mice (a gift from Dr. Schweitzer at Shriners Hospitals for Children), and Myf5-Cre mice (Jackson Laboratory stock# 007893). Cre-loxp recombination was induced by treatment with tamoxifen (100 mg/kg body weight, injected over five consecutive days) at 6 weeks

of age. Gain-of-function *Piezo1* mice were generated and maintained on a C57BL/6 background. All animals were backcrossed for at least 10 generations in C57BL/6 mice. The mice were housed under a 12-h light/dark cycle (light from 6 am to 6 pm) in a temperature-controlled room (24 °C) with free access to food and water. The age and sex of mice are described in the following sections. Experiments were performed using matched littermates. The PCR primer sequences used for genotyping are listed in **table S2**. All animal experiments were performed with the approval of the Scripps Institutional Animal Care and Use Committee. (Protocol No: IACUC-09-0029)

Human patellar tendon and joint samples

The human patellar tendon samples were derived from human knee joints. Samples were obtained from three tissue banks with the approval of the Scripps Human Subjects Committee (Protocol No: IRB-20-7636). Knee joints were processed within 72 h post-mortem. Joints were obtained from five young healthy donors (mean ± SD age, 31 ± 10.2 years; range, 20–41 years; four men and one woman). Tendons were used for tenocyte isolation.

Human genome samples

DNA samples used in this study were collected from previous studies (*15, 16*). The previous study was approved by the local ethics committees of the University of West Indies in Jamaica (Protocol: ECP 121). After providing informed consent, the participants were asked to complete a simple questionnaire detailing athletic achievement (if any) and their place of birth. Individuals born outside of the country were excluded from the study. After applying the exclusion criteria, elite athletes from around the entire island of Jamaica were sampled either during training or at home. Jamaican athletes who competed in international sprint events (100–400 m, jump, and throw) were

500 defined as elite athletes. For comparison, Jamaican controls representative of the Jamaican
501 population in their geographical distribution throughout the country, studying at the University of
502 the West Indies, were also included. The analysis was performed on DNA samples stored at
503 Juntendo University (Protocol ID: GSHSS31-93) and sent to Tokyo Medical and Dental University
504 (Protocol ID: G2020-033). This study was conducted in accordance with the principles of the
505 Declaration of Helsinki.
506
507 **Genotyping E756del carriers using sequencing**
508 The human genome samples were used for sequencing. A 200-bp PCR amplicon containing the
509 E756 locus was generated to sequence the E756del or wild-type allele (forward primer: 5'-
510 CAGGCAGGATGCAGTGAGTG-3'; reverse primer: 5'-GGACATGGCACAGCAGACTG-3').
511 Reverse primers were used for the sequencing.
512
513 **Mouse and human tenocytes isolation and cell culture**
514 *Mouse tenocyte isolation*
515 The mice were euthanized by cervical dislocation, and the Achilles tendons were dissected. The
516 tendons were trimmed on a clean bench to obtain tissue pieces. These tissues were incubated with
517 2.5% liberase-DL (5466202001, Sigma-Aldrich) for 45 min in a shaker (200 rpm, 37 °C). Isolated
518 cells were grown in α-modified eagle medium (α-MEM) with 10% fetal bovine serum (FBS)
519 and 1% penicillin-streptomycin (PS) until day 5, when the medium was replaced with fresh
520 medium. The cells were retrieved from passage one and used in the experiments. All cells were
521 cultured at 37 °C in a 5% CO_2 atmosphere.
522 *Human tenocyte isolation*

Patellar tendons were trimmed on a clean bench and cut into pieces. These tissues were incubated with 2.5% liberase-DL (5466202001, Sigma-Aldrich) for 8 h in a shaker (200 rpm, 37 °C). Isolated cells were grown in α-MEM with 10% FBS and 1% PS until day 5, when the medium was replaced with fresh medium. The cells were retrieved from passage one and used in the experiments. All cells were cultured at 37 °C in a 5% CO_2 atmosphere.

Calcium assay

Mouse and human tenocytes were used in the present study. After seeding (6 x 10^4 cells/well) and growing the cells in 96-well plates for 12 hours, Fluo-8 (ab112129; Abcam) was added according to the manufacturer's instructions. The Yoda1-induced amplitude change in the 485/538 fluorescence ratio was calculated by subtracting the baseline ratio prior to Yoda1 application. Yoda1 (SML1558, Sigma-Aldrich) was solubilized in DMSO as a stock solution of 50 mM and diluted to a final concentration of 3.125, 6.25, 12.5, 25, or 50 μM using Ca^{2+} imaging buffer for mouse cells, and diluted to a final concentration of 1, 5, 20, or 50 μM using Ca^{2+} imaging buffer for human cells.

Small molecule treatment in human tenocytes

After seeding cells (1.25 x 10^5 cells) and growing them in a 4 cm^2 stretch chamber (SC4D, Menicon Life Science) for 12 hours (70-80% confluency), PIEZO1 agonist (Yoda1, 25 μM, SML1558, Sigma-Aldrich, USA) or cyclosporin A (100 ng/mL, C-6000, LC Laboratories) was added to the cell culture medium. Mechanical stimuli were applied with an FX-5000 tissue tension system (Shellpa Pro, Menicon Life Science) at 2% stretch magnitudes and 0.25 Hz frequencies for

12 h in an incubator at 5% CO_2 and 37 °C. After mechanical stimulation, the cells were collected and used for qPCR.

Transfection in human tenocytes

After the cells attached to a 4 cm^2 stretch chamber (SC4D, Menicon Life Science) and formed a monolayer with 70-80% confluency, siRNA-mediated NFATC knockdown (SiControl; SIC001, SiNFTAC1; SASI_Hs01_0034-1013, SiNFTAC2; SASI_Hs01_0019-5473, SiNFTAC3; SASI_Hs01_0024-3957, SiNFTAC4; SASI_Hs01_0013-8884, Silencer Select, Millipore Sigma) was performed using Lipofectamine RNAi-MAX (13778100, Life Technologies) according to the manufacturer's instructions. After 48 h, mechanical stimuli were applied with an FX-5000 tissue tension system (Shellpa Pro, Menicon Life Science) at 2% stretch magnitudes and 0.25 Hz frequencies for 12 h in an incubator at 5% CO_2 and 37 °C. After mechanical stimulation, the cells were collected and used for qPCR.

Immunocytochemistry

After the cells attached to 96-well plate, DMSO or PIEZO1 agonist (Yoda1, 25 μM, SML1558, Sigma-Aldrich) treatment was performed. After 4 h, cells were fixed with 4% Paraformaldehyde/ phosphate-buffered saline (PFA/PBS) for 15 min. The cells were blocked with 5% bovine serum albumin (BSA) and 0.8% Triton X-100 in PBS for 2 h at 16 °C. Cells were incubated with primary antibodies in 1% BSA, 0.8% Triton X-100, 10% DMSO in PBS at 4 °C overnight. After the cells were washed with PBS three times for 5 min each, they were incubated with secondary antibodies for 1 h at 16 °C. After washing with PBS three times for 15 min, we evaluated the cells using a Keyence BZX700 widefield fluorescence microscope. The antibodies used in this experiment were

as follows: Anti-NFATC1 (1:100, sc-7294, Santa Cruz), Anti-NFATC2 (1:100, 8032S, Cell Signaling), Anti-NFATC3 (1:100, sc-8405, Santa Cruz), Anti- NFTAC4 (1:100, ab62613, Abcam), Alexa Fluor 488 conjugate (1:500, A11034 and A21121, Invitrogen, B13423), and Hoechst (1:5000, 33342, Invitrogen). ImageJ software was used to measure cell signal intensity (these were measured three times using different views).

Real time quantitative PCR

Total RNA from the Achilles tendons of mice and human tenocytes was isolated using the Zymo Direct-zol RNA MicroPrep kit (R2061, Zymo Research) according to the manufacturer's instructions. For reverse transcription, cDNA was synthesized using a PrimeScript RT Reagent Kit (RR037B, Takara Bio). Real-time PCR (RT-qPCR) was performed using a LightCycler 96 System (Roche Life Science, Indianapolis, IN) with custom primers (**tables S3 and 4**). The data were normalized to housekeeping genes or endogenous reference genes such as GAPDH.

RNA-seq

Total RNA from Achilles tendons of 18-week-old WT and *Piezo1* $^{tendon\text{-}mut/+}$ mice was used (n = 3 per group). RNA-Seq libraries were prepared using the GenNext RamDA-seq Single Cell Kit with NSR primers (Toyobo). Sequencing was performed using Illumina NextSeq 500 (paired-end, 37 cycle sequencing). Reads were aligned to the mouse genome (mm10) using STAR v2.7.6a. RSEM (v1.3.3) was used for read counting and generation of the count matrix. Differentially expressed genes were analyzed using edgeR (v3.32.1).

Single-cell RNA-seq

The Achilles tendons of 2-week-old WT mice were treated with 2.5% Liberase-DL (5466202001, Sigma-Aldrich) for 45 min in a shaker (200 rpm, 37 °C) and processed for single-cell sequencing using the Chromium Next GEM Single Cell 3' Reagent Kit v3.1 (10×Genomics). Libraries were sequenced using HighSeq X, and the resulting reads were mapped to the reference genome (mouse mm10) using CellRanger. Seurat (v4.0.0) was used for gene expression normalization and quantification, cell clustering, and visualization of gene expression in each cluster.

Long jump test

Piezo1 $^{systemic\text{-}mut/+}$, *Piezo1* $^{tendon\text{-}mut/+}$, *Piezo1* $^{muscle\text{-}mut/+}$ mice, and *Piezo1* $^{postnatal\text{-}tendon\text{-}mut/+}$ mice (12 weeks old) were used (n = 10 for each strain and sex). An empty cage was placed on the table of a beam raised 80 cm above the ground. Sufficient soft bedding and feed were placed in the cage to provide an optimum environment for the mice. To prevent injury and escape if the mice fell, a large plastic box was placed below the beam, and a soft substrate and soft cushions were placed in the box to cushion the fall. Before the beginning of the session, the beam was placed such that it touched the cage. After checking that the mice could walk from the beam into the cage, the horizontal distance between the cage and the beam was slowly increased by moving the beam farther away from the cage in 5-cm increments. Success rate and jump latency were measured at 10, 15, 20, 25, 30, 35, 40, 45, 50, 55, and 60 cm distances between beam and cage. Experiments at each distance were performed three times, and the distance was judged as “possible” if the mice could jump the distance 2 times. If the mice were unwilling to jump, the distance was judged as “not possible.” If the mice could not jump a particular distance, experiments with longer distances were not performed. This procedure was performed by two researchers, and the maximum jump distance of each mouse was considered for the analysis.

614

615 **Run-to-exhaustion test**

616 *Piezo1* $^{systemic\text{-}mut/+}$, *Piezo1* $^{tendon\text{-}mut/+}$, *Piezo1* $^{muscle\text{-}mut/+}$ mice, and *Piezo1* $^{postnatal\text{-}tendon\text{-}mut/+}$ mice were
617 used (n = 10 for each strain and sex). At the beginning of the experiment, the mice were started
618 running on a treadmill at a speed of 10 m/min. When the mouse reached the top of the belt, it was
619 considered to have acclimated to that speed, and the speed was increased by 1 m/min about every 2
620 min. Thus, we determined the maximum speed at which each mouse could acclimate. Immediately
621 after the maximum speed was determined, we continued the running test at this speed until
622 exhaustion occurred. Exhaustion is defined as stopping three times in a row and not resuming
623 running despite gentle encouragement (lightly pressing the buttocks with a tongue depressor) and
624 physical signs of exhaustion such as breathlessness and postural disturbances. If fatigue was
625 observed, mice were returned to their cages. This procedure was performed only once per mouse by
626 two researchers and the maximum speed was used as the result.

627

628 **High-speed video camera analysis**

629 WT and *Piezo1* $^{tendon\text{-}mut/+}$ mice were used (18 weeks old; n = 10 for each strain; male). In the
630 jumping analysis, the tail ridge of the mouse was used as a marker. For the analysis of ankle joint
631 motion, the right hind limbs of mice were shaved, and three anatomical landmarks (the lower third
632 of the tibia, fibula epiphysis, and fifth metatarsal head) were marked with a black ink marker (*40*).
633 The ankle joint angle was defined as the angle between the three markers. Movements of the right
634 hind limb markers were recorded during the jump test using a high-speed digital image camera
635 (iPhone 8) at 240 images/s. Tracker (https://physlets.org/tracker/) was used to identify markers for
636 assessment.

Statistical analysis

All data are presented as the mean ± s.e.m. or SD and represent at least 3 independent experiments. Statistical analyses, significance levels, and n values are described in the figures or figure legends. For the mouse experiments, n = number of animals, and at least three mice were used. For sample size determination, we performed power analysis using G*Power and repeatedly performed post-hoc analysis. In animal experiments, if mice refused to perform the long jump test and no data were obtained, the data from these mice were excluded from the analysis of all experiments. For comparisons between strains, we performed a two-tailed Student's t-test, Mann-Whitney test, Tukey's multiple comparisons test, Dunn's multiple comparisons test, and Fisher's exact test, where $P < 0.05$ was considered statistically significant. *$P < 0.05$. **$P < 0.01$. ***$P < 0.001$. ****$P < 0.0001$. For all datasets, statistical analysis was performed using Prism9. Individual subject-level data are reported in data file S1.

List of Supplementary Materials

Figs. S1to S11

Tables S1 to S4

MDAR Reproducibility Checklist

Movie S1

Data file S1

Acknowledgments:

We thank Dr. Ronen Schweitzer for sharing Scx-creERT2 mice; Dr. Hiroki Tsutsumi, Dr. Takehito Hananouchi, Dr. Kimberly Vanderpool, and Dr. Kathryn Spencer for technical support; Dr. Kenji

Kobayashi, Dr. Masashi Tanaka, Dr. Jian Ping Gong, and all the Asahara Lab members for their helpful discussions; and Dr. Helen Pickersgill at Life Science Editors for scientific critical reading and editorial assistance.

Funding:

AMED-CREST from AMED (Japan Agency for Medical Research and Development) (JP20gm0810008 to H.A.)

JSPS KAKENHI (Grant numbers: 19KK0227 and 20H05696 to H.A.)

National Institutes of Health (Grant numbers: AR050631 and AR065379 to H.A.)

Author contributions:

Research design: R.N., S.M. A.P., and H.A.

Biomechanical study: R.N. and T.N.

RNA seq and scRNA seq: R.N. and T.C.

Human genome study: R.N., R.K., G.W., and N.F.

Mice in vivo study: R.N. and H.O.

Histological study: R.N. and M.O.

Provision of resources: C.S., N.F., G.W., Y.P.P. M.L., and A.P.

Supervision: T.O., A.P., and H.A.

Data analysis: R.N., S.M., T.N., T.C., R.K. D.D.L, and H.A.

Writing the manuscript: R.N. and H.A.

Comments/feedback from all authors has been taken into account, and the final version agreed upon.

683

684 **Competing interests:**

685 All authors declare no competing interests.

686

687 **Data and materials availability:**

688 All data required to reproduce this study are included in this published article and supplementary
689 information. Raw RNA-seq data were deposited in GEO under accession number GSE169261.
690 Single-cell RNA-seq data were deposited in the DDBJ under the accession number DRA013310.
691 Further information and requests for resources and reagents should be directed to and will be
692 fulfilled by the authors.

693

References and Notes

1. T. J. Dawson, C. R. Taylor, Energetic Cost of Locomotion in Kangaroos. *Nature* **246**, 313-314 (1973).
2. D. L. Morgan, U. Proske, D. Warren, Measurements of muscle stiffness and the mechanism of elastic storage of energy in hopping kangaroos. *J Physiol* **282**, 253-261 (1978).
3. A. Biewener, R. Baudinette, In vivo muscle force and elastic energy storage during steady-speed hopping of tammar wallabies (Macropus eugenii). *J Exp Biol* **198**, 1829-1841 (1995).
4. A. V. Hill, The heat of shortening and the dynamic constants of muscle. *Proceeding of the Royal Sciety of London* **B126**, 136-195 (1938).
5. K. T. Palomares, R. E. Gleason, Z. D. Mason, D. M. Cullinane, T. A. Einhorn, L. C. Gerstenfeld, E. F. Morgan, Mechanical stimulation alters tissue differentiation and molecular expression during bone healing. *J Orthop Res* **27**, 1123-1132 (2009).
6. G. Candiani, S. A. Riboldi, N. Sadr, S. Lorenzoni, P. Neuenschwander, F. M. Montevecchi, S. Mantero, Cyclic mechanical stimulation favors myosin heavy chain accumulation in engineered skeletal muscle constructs. *J Appl Biomater Biomech* **8**, 68-75 (2010).
7. M. Khoshgoftar, C. C. van Donkelaar, K. Ito, Mechanical stimulation to stimulate formation of a physiological collagen architecture in tissue-engineered cartilage: a numerical study. *Comput Methods Biomech Biomed Engin* **14**, 135-144 (2011).
8. P. Eliasson, A. Fahlgren, B. Pasternak, P. Aspenberg, Unloaded rat Achilles tendons continue to grow, but lose viscoelasticity. *J Appl Physiol (1985)* ***103***, 459-463 (2007).

9. H. Langberg, L. Rosendal, M. Kjaer, Training-induced changes in peritendinous type I collagen turnover determined by microdialysis in humans. *J Physiol* **534**, 297-302 (2001).
10. H. Langberg, H. Ellingsgaard, T. Madsen, J. Jansson, S. P. Magnusson, P. Aagaard, M. Kjaer, Eccentric rehabilitation exercise increases peritendinous type I collagen synthesis in humans with Achilles tendinosis. *Scand J Med Sci Sports* **17**, 61-66 (2007).
11. T. Wang, Z. Lin, M. Ni, C. Thien, R. E. Day, B. Gardiner, J. Rubenson, T. B. Kirk, D. W. Smith, A. Wang, D. G. Lloyd, Y. Wang, Q. Zheng, M. H. Zheng, Cyclic mechanical stimulation rescues achilles tendon from degeneration in a bioreactor system. *J Orthop Res* **33**, 1888-1896 (2015).
12. R. R. Suminski, C. O. Mattern, S. T. Devor, Influence of racial origin and skeletal muscle properties on disease prevalence and physical performance. *Sports Med* **32**, 667-673 (2002).
13. T. Ceaser, G. Hunter, Black and White race differences in aerobic capacity, muscle fiber type, and their influence on metabolic processes. *Sports Med* **45**, 615-623 (2015).
14. Y. P. Pitsiladis, M. Tanaka, N. Eynon, C. Bouchard, K. N. North, A. G. Williams, M. Collins, C. N. Moran, S. L. Britton, N. Fuku, E. A. Ashley, V. Klissouras, A. Lucia, Ahmetov, II, E. de Geus, M. Alsayrafi, Athlome Project Consortium: a concerted effort to discover genomic and other "omic" markers of athletic performance. *Physiol Genomics* **48**, 183-190 (2016).
15. R. A. Scott, R. Irving, L. Irwin, E. Morrison, V. Charlton, K. Austin, D. Tladi, M. Deason, S. A. Headley, F. W. Kolkhorst, N. Yang, K. North, Y. P. Pitsiladis, ACTN3 and ACE genotypes in elite Jamaican and US sprinters. *Med Sci Sports Exerc* **42**, 107-112 (2010).

16. M. Deason, R. Scott, L. Irwin, V. Macaulay, N. Fuku, M. Tanaka, R. Irving, V. Charlton, E. Morrison, K. Austin, Y. P. Pitsiladis, Importance of mitochondrial haplotypes and maternal lineage in sprint performance among individuals of West African ancestry. *Scand J Med Sci Sports* **22**, 217-223 (2012).
17. B. Coste, J. Mathur, M. Schmidt, T. J. Earley, S. Ranade, M. J. Petrus, A. E. Dubin, A. Patapoutian, Piezo1 and Piezo2 are essential components of distinct mechanically activated cation channels. *Science* **330**, 55-60 (2010).
18. B. Coste, B. Xiao, J. S. Santos, R. Syeda, J. Grandl, K. S. Spencer, S. E. Kim, M. Schmidt, J. Mathur, A. E. Dubin, M. Montal, A. Patapoutian, Piezo proteins are pore-forming subunits of mechanically activated channels. *Nature* **483**, 176-181 (2012).
19. J. Li, B. Hou, S. Tumova, K. Muraki, A. Bruns, M. J. Ludlow, A. Sedo, A. J. Hyman, L. McKeown, R. S. Young, N. Y. Yuldasheva, Y. Majeed, L. A. Wilson, B. Rode, M. A. Bailey, H. R. Kim, Z. Fu, D. A. Carter, J. Bilton, H. Imrie, P. Ajuh, T. N. Dear, R. M. Cubbon, M. T. Kearney, R. K. Prasad, P. C. Evans, J. F. Ainscough, D. J. Beech, Piezo1 integration of vascular architecture with physiological force. *Nature* **515**, 279-282 (2014).
20. K. Nonomura, V. Lukacs, D. T. Sweet, L. M. Goddard, A. Kanie, T. Whitwam, S. S. Ranade, T. Fujimori, M. L. Kahn, A. Patapoutian, Mechanically activated ion channel PIEZO1 is required for lymphatic valve formation. *Proc Natl Acad Sci U S A* **115**, 12817-12822 (2018).
21. X. Li, L. Han, I. Nookaew, E. Mannen, M. J. Silva, M. Almeida, J. Xiong, Stimulation of Piezo1 by mechanical signals promotes bone anabolism. *Elife* **8**, (2019).

22. W. Sun, S. Chi, Y. Li, S. Ling, Y. Tan, Y. Xu, F. Jiang, J. Li, C. Liu, G. Zhong, D. Cao, X. Jin, D. Zhao, X. Gao, Z. Liu, B. Xiao, Y. Li, The mechanosensitive Piezo1 channel is required for bone formation. *Elife* **8**, (2019).
23. T. Zhou, B. Gao, Y. Fan, Y. Liu, S. Feng, Q. Cong, X. Zhang, Y. Zhou, P. S. Yadav, J. Lin, N. Wu, L. Zhao, D. Huang, S. Zhou, P. Su, Y. Yang, Piezo1/2 mediate mechanotransduction essential for bone formation through concerted activation of NFAT-YAP1-ß-catenin. *Elife* **9**, (2020).
24. W. Lee, H. A. Leddy, Y. Chen, S. H. Lee, N. A. Zelenski, A. L. McNulty, J. Wu, K. N. Beicker, J. Coles, S. Zauscher, J. Grandl, F. Sachs, F. Guilak, W. B. Liedtke, Synergy between Piezo1 and Piezo2 channels confers high-strain mechanosensitivity to articular cartilage. *Proc Natl Acad Sci U S A* **111**, E5114-5122 (2014).
25. M. R. Servin-Vences, M. Moroni, G. R. Lewin, K. Poole, Direct measurement of TRPV4 and PIEZO1 activity reveals multiple mechanotransduction pathways in chondrocytes. *Elife* **6**, (2017).
26. W. Lee, R. J. Nims, A. Savadipour, Q. Zhang, H. A. Leddy, F. Liu, A. L. McNulty, Y. Chen, F. Guilak, W. B. Liedtke, Inflammatory signaling sensitizes Piezo1 mechanotransduction in articular chondrocytes as a pathogenic feed-forward mechanism in osteoarthritis. *Proc Natl Acad Sci U S A* **118**, (2021).
27. R. Zarychanski, V. P. Schulz, B. L. Houston, Y. Maksimova, D. S. Houston, B. Smith, J. Rinehart, P. G. Gallagher, Mutations in the mechanotransduction protein PIEZO1 are associated with hereditary xerocytosis. *Blood* **120**, 1908-1915 (2012).
28. J. Albuisson, S. E. Murthy, M. Bandell, B. Coste, H. Louis-Dit-Picard, J. Mathur, M. Feneant-Thibault, G. Tertian, J. P. de Jaureguiberry, P. Y. Syfuss, S. Cahalan, L. Garcon,

F. Toutain, P. Simon Rohrlich, J. Delaunay, V. Picard, X. Jeunemaitre, A. Patapoutian, Dehydrated hereditary stomatocytosis linked to gain-of-function mutations in mechanically activated PIEZO1 ion channels. *Nat Commun* **4**, 1884 (2013).

29. C. Bae, R. Gnanasambandam, C. Nicolai, F. Sachs, P. A. Gottlieb, Xerocytosis is caused by mutations that alter the kinetics of the mechanosensitive channel PIEZO1. *Proc Natl Acad Sci U S A* **110**, E1162-1168 (2013).

30. V. Lukacs, J. Mathur, R. Mao, P. Bayrak-Toydemir, M. Procter, S. M. Cahalan, H. J. Kim, M. Bandell, N. Longo, R. W. Day, D. A. Stevenson, A. Patapoutian, B. L. Krock, Impaired PIEZO1 function in patients with a novel autosomal recessive congenital lymphatic dysplasia. *Nat Commun* **6**, 8329 (2015).

31. S. Ma, S. Cahalan, G. LaMonte, N. D. Grubaugh, W. Zeng, S. E. Murthy, E. Paytas, R. Gamini, V. Lukacs, T. Whitwam, M. Loud, R. Lohia, L. Berry, S. M. Khan, C. J. Janse, M. Bandell, C. Schmedt, K. Wengelnik, A. I. Su, E. Honore, E. A. Winzeler, K. G. Andersen, A. Patapoutian, Common PIEZO1 Allele in African Populations Causes RBC Dehydration and Attenuates Plasmodium Infection. *Cell* **173**, 443-455.e412 (2018).

32. S. Ma, A. E. Dubin, Y. Zhang, S. A. R. Mousavi, Y. Wang, A. M. Coombs, M. Loud, I. Andolfo, A. Patapoutian, A role of PIEZO1 in iron metabolism in mice and humans. *Cell* **184**, 969-982.e913 (2021).

33. F. S. Passini, P. K. Jaeger, A. S. Saab, S. Hanlon, N. A. Chittim, M. J. Arlt, K. D. Ferrari, D. Haenni, S. Caprara, M. Bollhalder, B. Niederöst, A. N. Horvath, T. Götschi, S. Ma, B. Passini-Tall, S. F. Fucentese, U. Blache, U. Silván, B. Weber, K. G. Silbernagel, J. G. Snedeker, Shear-stress sensing by PIEZO1 regulates tendon stiffness in rodents and influences jumping performance in humans. *Nat Biomed Eng*, (2021).

34. N. Mittal, J. Pan, J. Palmateer, L. Martin, A. Pandya, S. Kumar, A. Ofomata, P. D. Hurn, T. Schallert, So you think you can jump? A novel long jump assessment to detect deficits in stroked mice. *J Neurosci Methods* **256**, 212-219 (2015).

35. J. D. Conner, T. Wolden-Hanson, L. S. Quinn, Assessment of murine exercise endurance without the use of a shock grid: an alternative to forced exercise. *J Vis Exp*, e51846 (2014).

36. P. Cserjesi, D. Brown, K. L. Ligon, G. E. Lyons, N. G. Copeland, D. J. Gilbert, N. A. Jenkins, E. N. Olson, Scleraxis: a basic helix-loop-helix protein that prefigures skeletal formation during mouse embryogenesis. *Development* **121**, 1099-1110 (1995).

37. R. Schweitzer, J. H. Chyung, L. C. Murtaugh, A. E. Brent, V. Rosen, E. N. Olson, A. Lassar, C. J. Tabin, Analysis of the tendon cell fate using Scleraxis, a specific marker for tendons and ligaments. *Development* **128**, 3855-3866 (2001).

38. Y. Ito, N. Toriuchi, T. Yoshitaka, H. Ueno-Kudoh, T. Sato, S. Yokoyama, K. Nishida, T. Akimoto, M. Takahashi, S. Miyaki, H. Asahara, The Mohawk homeobox gene is a critical regulator of tendon differentiation. *Proc Natl Acad Sci U S A* **107**, 10538-10542 (2010).

39. W. Liu, S. S. Watson, Y. Lan, D. R. Keene, C. E. Ovitt, H. Liu, R. Schweitzer, R. Jiang, The atypical homeodomain transcription factor Mohawk controls tendon morphogenesis. *Mol Cell Biol* **30**, 4797-4807 (2010).

40. R. Syeda, J. Xu, A. E. Dubin, B. Coste, J. Mathur, T. Huynh, J. Matzen, J. Lao, D. C. Tully, I. H. Engels, H. M. Petrassi, A. M. Schumacher, M. Montal, M. Bandell, A.

Patapoutian, Chemical activation of the mechanotransduction channel Piezo1. *Elife* **4**, (2015).

41. D. Dayan, Y. Hiss, A. Hirshberg, J. J. Bubis, M. Wolman, Are the polarization colors of picrosirius red-stained collagen determined only by the diameter of the fibers? *Histochemistry* **93**, 27-29 (1989).

42. H. Trau, D. Dayan, A. Hirschberg, Y. Hiss, J. J. Bubis, M. Wolman, Connective tissue nevi collagens. Study with picrosirius red and polarizing microscopy. *Am J Dermatopathol* **13**, 374-377 (1991).

43. H. Liu, C. Zhang, S. Zhu, P. Lu, T. Zhu, X. Gong, Z. Zhang, J. Hu, Z. Yin, B. C. Heng, X. Chen, H. W. Ouyang, Mohawk promotes the tenogenesis of mesenchymal stem cells through activation of the TGFβ signaling pathway. *Stem Cells* **33**, 443-455 (2015).

44. R. Nakamichi, Y. Ito, M. Inui, N. Onizuka, T. Kayama, K. Kataoka, H. Suzuki, M. Mori, M. Inagawa, S. Ichinose, M. K. Lotz, D. Sakai, K. Masuda, T. Ozaki, H. Asahara, Mohawk promotes the maintenance and regeneration of the outer annulus fibrosus of intervertebral discs. *Nat Commun* **7**, 12503 (2016).

45. X. Chen, Z. Yin, J. L. Chen, H. H. Liu, W. L. Shen, Z. Fang, T. Zhu, J. Ji, H. W. Ouyang, X. H. Zou, Scleraxis-overexpressed human embryonic stem cell-derived mesenchymal stem cells for tendon tissue engineering with knitted silk-collagen scaffold. *Tissue Eng Part A* **20**, 1583-1592 (2014).

46. A. Rao, NF-ATp: a transcription factor required for the co-ordinate induction of several cytokine genes. *Immunology today* **15**, 274-281 (1994).

47. P. G. Hogan, L. Chen, J. Nardone, A. Rao, Transcriptional regulation by calcium, calcineurin, and NFAT. *Genes & development* **17**, 2205-2232 (2003).

48. T. Strasmann, E. Weihe, Z. Halata, CGRP-like immunoreactivity in sensory nerve endings of the Golgi tendon organ. A light- and electron-microscopic study in the grey short-tailed opossum (Monodelphis domestica). *Acta Anat (Basel)* **137**, 278-281 (1990).

49. R. W. Norman, P. V. Komi, Electromechanical delay in skeletal muscle under normal movement conditions. *Acta Physiol Scand* **106**, 241-248 (1979).

50. R. M. Alexander, Optimum take-off techniques for high and long jumps. *Philos Trans R Soc Lond B Biol Sci* **329**, 3-10 (1990).

51. A. Seyfarth, A. Friedrichs, V. Wank, R. Blickhan, Dynamics of the long jump. *J Biomech* **32**, 1259-1267 (1999).

52. A. Iwata, S. Fuchioka, K. Hiraoka, M. Masuhara, K. Kami, Characteristics of locomotion, muscle strength, and muscle tissue in regenerating rat skeletal muscles. *Muscle Nerve* **41**, 694-701 (2010).

53. C. N. Maganaris, J. P. Paul, In vivo human tendon mechanical properties. *J Physiol* ***521*** *Pt* 1, 307-313 (1999).

54. J. H. Wang, Mechanobiology of tendon. *J Biomech* 39, 1563-1582 (2006).

55. A. J. Bayliss, A. M. Weatherholt, T. T. Crandall, D. L. Farmer, J. C. McConnell, K. M. Crossley, S. J. Warden, Achilles tendon material properties are greater in the jump leg of jumping athletes. *J Musculoskelet Neuronal Interact* **16**, 105-112 (2016).

56. M. Abrahams, Mechanical behaviour of tendonIn vitro. *Medical and biological engineering* **5**, 433-443 (1967).

57. A. J. Bayliss, A. M. Weatherholt, T. T. Crandall, D. L. Farmer, J. C. McConnell, K. M. Crossley, S. J. Warden, Achilles tendon material properties are greater in the jump leg of jumping athletes. J Musculoskelet Neuronal Interact 16, 105-112 (2016).

875 58. K. Kubo, M. Morimoto, T. Komuro, H. Yata, N. Tsunoda, H. Kanehisa, T. Fukunaga,
876 Effects of plyometric and weight training on muscle-tendon complex and jump
877 performance. Med Sci Sports Exerc 39, 1801-1810 (2007).
878 59. J. H. Wang, Mechanobiology of tendon. J Biomech 39, 1563-1582 (2006).
879
880 60. S. Agarwal, S. J. Loder, D. Cholok, J. Peterson, J. Li, C. Breuler, R. Cameron Brownley,
881 H. Hsin Sung, M. T. Chung, N. Kamiya, S. Li, B. Zhao, V. Kaartinen, T. A. Davis, A. T.
882 Qureshi, E. Schipani, Y. Mishina, B. Levi, Scleraxis-Lineage Cells Contribute to Ectopic
883 Bone Formation in Muscle and Tendon. *Stem Cells* **35**, 705-710 (2017).
884 61. K. T. Best, A. E. Loiselle, Scleraxis lineage cells contribute to organized bridging tissue
885 during tendon healing and identify a subpopulation of resident tendon cells. *Faseb j* **33**,
886 8578-8587 (2019).
887 62. T. Maeda, T. Sakabe, A. Sunaga, K. Sakai, A. L. Rivera, D. R. Keene, T. Sasaki, E.
888 Stavnezer, J. Iannotti, R. Schweitzer, D. Ilic, H. Baskaran, T. Sakai, Conversion of
889 mechanical force into TGF-β-mediated biochemical signals. *Curr Biol* **21**, 933-941
890 (2011).
891 63. T. Kayama, M. Mori, Y. Ito, T. Matsushima, R. Nakamichi, H. Suzuki, S. Ichinose, M.
892 Saito, K. Marumo, H. Asahara, Gtf2ird1-Dependent Mohawk Expression Regulates
893 Mechanosensing Properties of the Tendon. Mol Cell Biol **36**, 1297-1309 (2016).
894 64. P. V. Komi, Physiological and biomechanical correlates of muscle function: effects of
895 muscle structure and stretch-shortening cycle on force and speed. *Exerc Sport Sci Re*v **12**,
896 81-121 (1984).

65. C. Bosco, J. T. Viitasalo, P. V. Komi, P. Luhtanen, Combined effect of elastic energy and myoelectrical potentiation during stretch-shortening cycle exercise. *Acta Physiol Scand* **114**, 557-565 (1982).

66. C. Bosco, G. Montanari, R. Ribacchi, P. Giovenali, F. Latteri, G. Iachelli, M. Faina, R. Colli, A. Dal Monte, M. La Rosa, et al., Relationship between the efficiency of muscular work during jumping and the energetics of running. *Eur J Appl Physiol Occup Physiol* **56**, 138-143 (1987).

67. M. F. Bobbert, L. J. Casius, Is the effect of a countermovement on jump height due to active state development? *Med Sci Sports Exerc* **37**, 440-446 (2005).

68. K. A. Edman, G. Elzinga, M. I. Noble, Enhancement of mechanical performance by stretch during tetanic contractions of vertebrate skeletal muscle fibres. *J Physiol* **281**, 139-155 (1978).

69. G. J. Ettema, P. A. Huijing, A. de Haan, The potentiating effect of prestretch on the contractile performance of rat gastrocnemius medialis muscle during subsequent shortening and isometric contractions. *J Exp Biol* **165**, 121-136 (1992).

70. W. Herzog, R. Schachar, T. R. Leonard, Characterization of the passive component of force enhancement following active stretching of skeletal muscle. *J Exp Biol* **206**, 3635-3643 (2003).

71. K. Kubo, Y. Kawakami, T. Fukunaga, Influence of elastic properties of tendon structures on jump performance in humans. *J Appl Physiol (1985)* **87**, 2090-2096 (1999).

72. T. Finni, S. Ikegawa, P. V. Komi, Concentric force enhancement during human movement. *Acta Physiol Scand* **173**, 369-377 (2001).

73. J. M. McBride, G. O. McCaulley, P. Cormie, Influence of preactivity and eccentric muscle activity on concentric performance during vertical jumping. *J Strength Cond Res* **22**, 750-757 (2008).
74. G. A. Lichtwark, A. M. Wilson, Effects of series elasticity and activation conditions on muscle power output and efficiency. *J Exp Biol* **208**, 2845-2853 (2005).
75. G. A. Lichtwark, C. J. Barclay, The influence of tendon compliance on muscle power output and efficiency during cyclic contractions. *J Exp Biol* **213**, 707-714 (2010).
76. C. T. Thorpe, H. L. Birch, P. D. Clegg, H. R. Screen, The role of the non-collagenous matrix in tendon function. *Int J Exp Pathol* **94**, 248-259 (2013).
77. C. T. Thorpe, K. J. Karunaseelan, J. Ng Chieng Hin, G. P. Riley, H. L. Birch, P. D. Clegg, H. R. Screen, Distribution of proteins within different compartments of tendon varies according to tendon type. *J Anat* **229**, 450-458 (2016).
78. T. Funakoshi, T. Schmid, H. P. Hsu, M. Spector, Lubricin distribution in the goat infraspinatus tendon: a basis for interfascicular lubrication. *J Bone Joint Surg Am* **90**, 803-814 (2008).
79. R. T. Kohrs, C. Zhao, Y. L. Sun, G. D. Jay, L. Zhang, M. L. Warman, K. N. An, P. C. Amadio, Tendon fascicle gliding in wild type, heterozygous, and lubricin knockout mice. *J Orthop Res* **29**, 384-389 (2011).
80. K. D. Smith, A. Vaughan-Thomas, D. G. Spiller, J. F. Innes, P. D. Clegg, E. J. Comerford, The organisation of elastin and fibrillins 1 and 2 in the cruciate ligament complex. *J Anat* **218**, 600-607 (2011).

81. J. Gosline, M. Lillie, E. Carrington, P. Guerette, C. Ortlepp, K. Savage, Elastic proteins: biological roles and mechanical properties. *Philos Trans R Soc Lond B Biol Sci* **357**, 121-132 (2002).

82. T. M. Ritty, K. Ditsios, B. C. Starcher, Distribution of the elastic fiber and associated proteins in flexor tendon reflects function. *Anat Rec* **268**, 430-440 (2002).

83. C. T. Thorpe, Extracellular Matrix Synthesis and Degradation in Functionally Distinct Tendons*, London: Institute of Orthopaedics and Musculoskeletal Science, University College London.* (2010).

84. R. K. Smith, M. Gerard, B. Dowling, A. J. Dart, H. L. Birch, A. E. Goodship, Correlation of cartilage oligomeric matrix protein (COMP) levels in equine tendon with mechanical properties: a proposed role for COMP in determining function-specific mechanical characteristics of locomotor tendons. *Equine Vet J Suppl*, 241-244 (2002).

85. J. Wang, M. Horlick, J. C. Thornton, L. S. Levine, S. B. Heymsfield, R. N. Pierson, Jr., Correlations between skeletal muscle mass and bone mass in children 6-18 years: influences of sex, ethnicity, and pubertal status. *Growth Dev Aging **63***, 99-109 (1999).

86. J. H. Himes, Racial variation in physique and body composition. *Can J Sport Sci **13***, 117-126 (1988).

87. T. Abe, J. B. Brown, W. F. Brechue, Architectural characteristics of muscle in black and white college football players. *Med Sci Sports Exerc **31***, 1448-1452 (1999).

88. K. N. North, N. Yang, D. Wattanasirichaigoon, M. Mills, S. Easteal, A. H. Beggs, A common nonsense mutation results in alpha-actinin-3 deficiency in the general population. *Nat Genet **21***, 353-354 (1999).

89. N. Yang, D. G. MacArthur, J. P. Gulbin, A. G. Hahn, A. H. Beggs, S. Easteal, K. North, ACTN3 genotype is associated with human elite athletic performance. *Am J Hum Genet* ***73***, 627-631 (2003).

90. A. K. Niemi, K. Majamaa, Mitochondrial DNA and ACTN3 genotypes in Finnish elite endurance and sprint athletes. *Eur J Hum Genet* ***13***, 965-969 (2005).

91. P. M. Clarkson, J. M. Devaney, H. Gordish-Dressman, P. D. Thompson, M. J. Hubal, M. Urso, T. B. Price, T. J. Angelopoulos, P. M. Gordon, N. M. Moyna, L. S. Pescatello, P. S. Visich, R. F. Zoeller, R. L. Seip, E. P. Hoffman, ACTN3 genotype is associated with increases in muscle strength in response to resistance training in women. *J Appl Physiol (1985)* ***99***, 154-163 (2005).

92. C. N. Moran, N. Yang, M. E. Bailey, A. Tsiokanos, A. Jamurtas, D. G. MacArthur, K. North, Y. P. Pitsiladis, R. H. Wilson, Association analysis of the ACTN3 R577X polymorphism and complex quantitative body composition and performance phenotypes in adolescent Greeks. *Eur J Hum Genet* **15**, 88-93 (2007).

93. D. G. MacArthur, J. T. Seto, J. M. Raftery, K. G. Quinlan, G. A. Huttley, J. W. Hook, F. A. Lemckert, A. J. Kee, M. R. Edwards, Y. Berman, E. C. Hardeman, P. W. Gunning, S. Easteal, N. Yang, K. N. North, Loss of ACTN3 gene function alters mouse muscle metabolism and shows evidence of positive selection in humans. *Nature Genetics* **39**, 1261-1265 (2007).

94. S. Myerson, H. Hemingway, R. Budget, J. Martin, S. Humphries, H. Montgomery, Human angiotensin I-converting enzyme gene and endurance performance. *J Appl Physiol (1985)* **87**, 1313-1316 (1999).

95. D. Woods, M. Hickman, Y. Jamshidi, D. Brull, V. Vassiliou, A. Jones, S. Humphries, H. Montgomery, Elite swimmers and the D allele of the ACE I/D polymorphism. *Hum Genet* **108**, 230-232 (2001).
96. G. Gayagay, B. Yu, B. Hambly, T. Boston, A. Hahn, D. S. Celermajer, R. J. Trent, Elite endurance athletes and the ACE I allele--the role of genes in athletic performance. *Hum Genet* **103**, 48-50 (1998).
97. R. Alvarez, N. Terrados, R. Ortolano, G. Iglesias-Cubero, J. R. Reguero, A. Batalla, A. Cortina, B. Fernández-García, C. Rodríguez, S. Braga, V. Alvarez, E. Coto, Genetic variation in the renin-angiotensin system and athletic performance. *Eur J Appl Physiol* **82**, 117-120 (2000).
98. N. L. Millar, G. A. Murrell, I. B. McInnes, Inflammatory mechanisms in tendinopathy - towards translation. *Nat Rev Rheumatol* **13**, 110-122 (2017).
99. A. E. C. Nichols, R. E. Settlage, S. R. Werre, L. A. Dahlgren, Novel roles for scleraxis in regulating adult tenocyte function. *BMC Cell Biol* **19**, 14 (2018).
100. H. Nakahara, A. Hasegawa, K. Otabe, F. Ayabe, T. Matsukawa, N. Onizuka, Y. Ito, T. Ozaki, M. K. Lotz, H. Asahara, Transcription factor Mohawk and the pathogenesis of human anterior cruciate ligament degradation. *Arthritis Rheum* **65**, 2081-2089 (2013).
101. C. Spang, J. Chen, L. J. Backman, The tenocyte phenotype of human primary tendon cells in vitro is reduced by glucocorticoids. *BMC Musculoskelet Disord* **17**, 467 (2016).

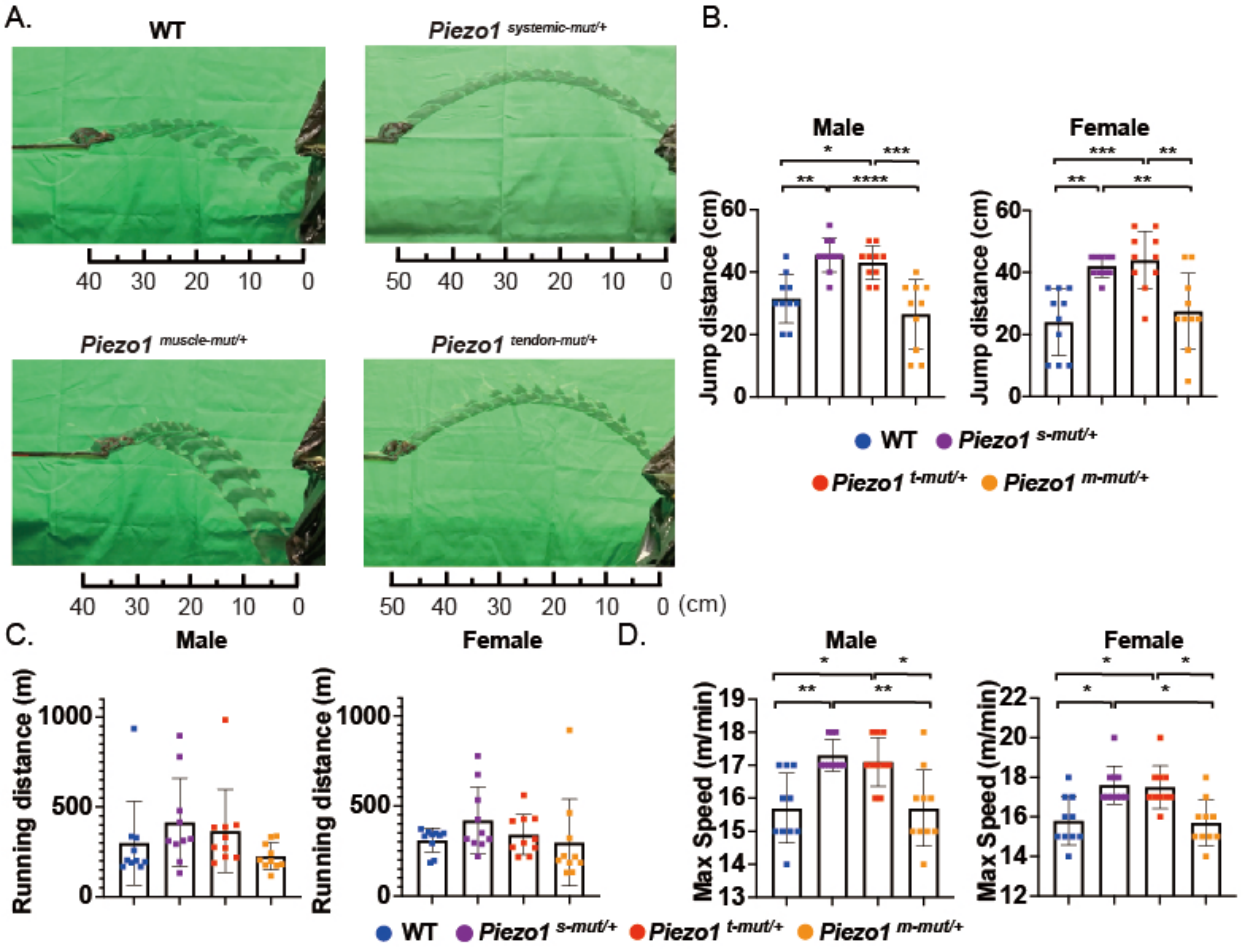

Fig. 1. Tendon-specific R2482H *Piezo1* enhances jumping power and maximum running speed in mice.

(**A**) Representative images of jumping in WT, *Piezo1*$^{systemic\text{-}mut/+}$, *Piezo1* $^{tendon\text{-}mut/+}$, and *Piezo1* $^{muscle\text{-}mut/+}$mice. (**B**) Maximum jumping distance of each mouse. Male and Female. n =10 of each. Error bars represent standard deviation (SD); * $P < 0.05$, ** $P < 0.01$, *** $P < 0.001$, **** $P < 0.0001$; Tukey's multiple comparisons test. (**C, D**) Running distance (C) and maximum running speed (D) during the run-to-exhaustion test in WT, *Piezo1* $^{systemic\text{-}mut/+}$, *Piezo1* $^{tendon\text{-}mut/+}$, and *Piezo1* $^{muscle\text{-}mut/+}$mice. n = 10. Error bars represent SD; * $P < 0.05$, ** $P < 0.01$; Dunn's multiple comparisons test.

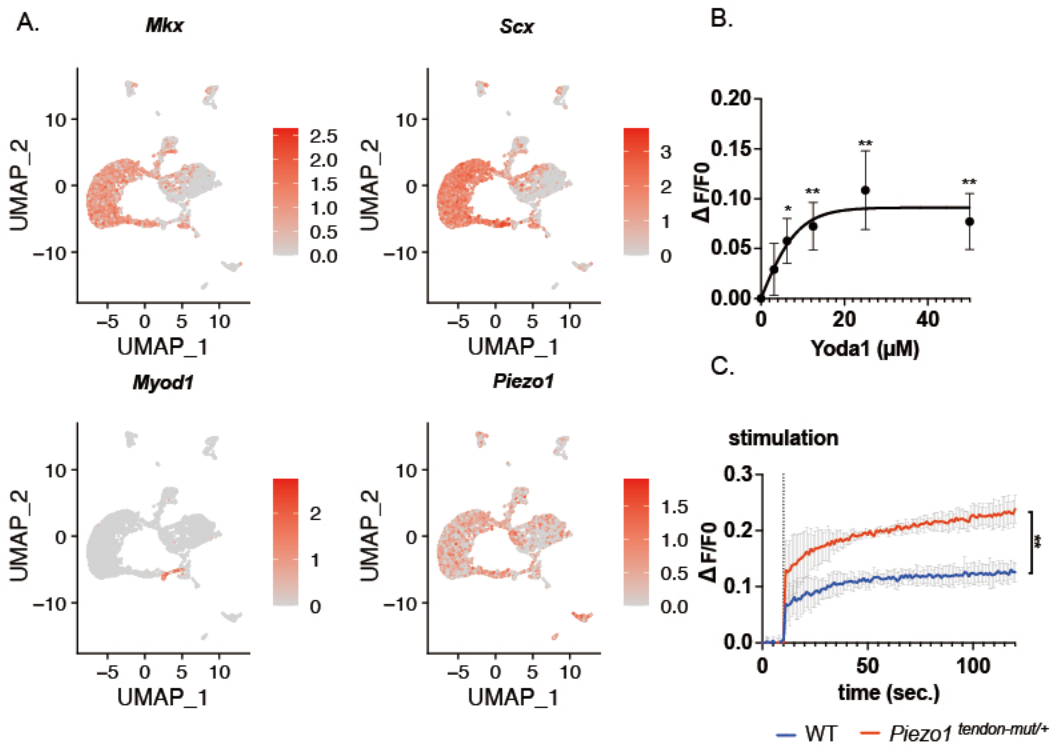

Fig. 2. PIEZO1 is a mechano-sensitive ion channel in tenocytes.
(**A**) Visualization of *Mkx*, *Scx*, *Myod1* and *Piezo1* on Uniform manifold Approximation and Projection (UMAP) of scRNA-seq data from fresh Achilles tendon-derived cells of 2-week-old mice. (**B**) Yoda1-induced intracellular calcium signals in mouse tenocyte in multiple dose conditions. Normalized using values without stimulation. n = 3. Error bars represent SD; * $P <$ 0.05, ** $P < 0.01$; unpaired Student's t-test. (**C**) Yoda1-induced intracellular calcium signals in mouse tenocytes of WT mice and *Piezo1* $^{tendon\text{-}mut/+}$ mice. The concentration of Yoda1 was 25 μM. Values were normalized to the value without stimulation. n = 3. Error bars represent SD, ** P <0.01, unpaired Student's t-test.

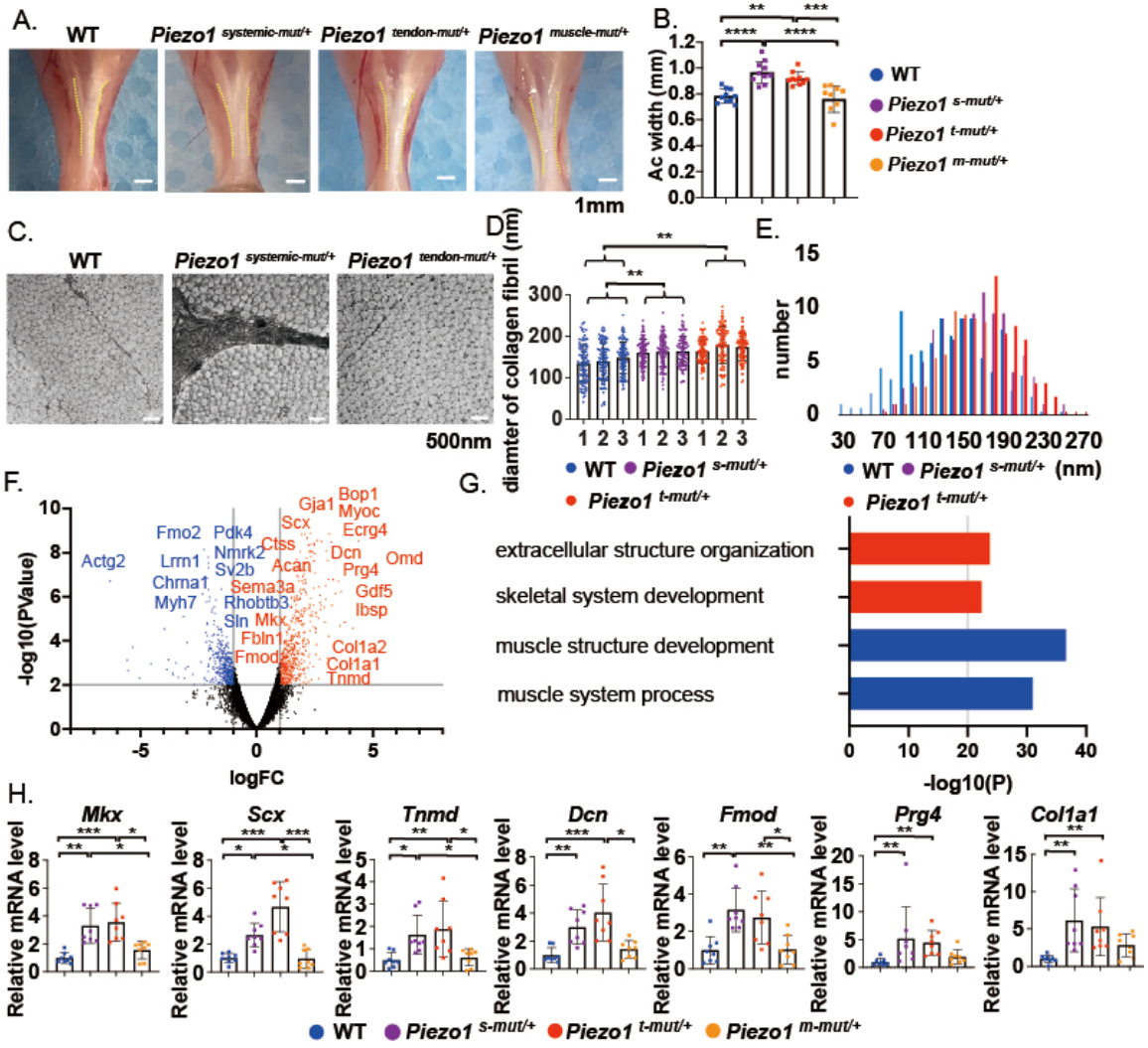

Fig. 3. Morphological and transcriptomic alteration via R2482H *Piezo1* in tenocytes.
(**A**) Representative images of the macroscopic views of the Achilles tendons of 18-week-old male mice. Scale bars, 1 mm. (**B**) Width of the Achilles tendon of 18-week-old mice. n = 10. Error bars represent SD; ** P <0.01, *** P <0.001, **** P <0.0001; Tukey's multiple comparisons test. (**C**) Representative images of transmission electron microscopy of the Achilles tendon of 18-week-old male mice. Scale bars, 500 nm. (**D**) The diameter of 100 collagen fibrils from these male mice. n = 3 of each. For WT mice, mean diameter = 140.6 nm. For *Piezo1* $^{s\text{-}mut/+}$ mice, mean diameter = 162.2 nm. For *Piezo1* $^{t\text{-}mut/+}$ mice, mean diameter = 172.3 nm. ** P < 0.01; Tukey's multiple comparisons test. (**E**) Histogram of the diameters of the collagen fibrils. Blue bar, WT mice; green bar, *Piezo1* $^{s\text{-}mut/+}$ mice; red bar, *Piezo1* $^{t\text{-}mut/+}$ mice. (**F**) Volcano plot of the differentially expressed genes between the tendons of WT mice vs *Piezo1* $^{t\text{-}mut/+}$ mice. Significantly upregulated genes are represented in red, significantly downregulated genes are in blue, non-significant genes are in black. Silver vertical lines highlight log fold changes of -1 and 1, whereas silver horizontal line represents -log10 (P-value) of 2. (**G**) Gene Ontology enrichment analysis of up- (red) and down- (blue) regulated genes in the tendons of *Piezo1* $^{t\text{-}mut/+}$ mice compared to WT mice. (**H**) qPCR analysis of the expression of tendon-related genes in the Achilles tendon of each 18-week-old mouse. n = 8. Error bars represent SD; * P < 0.05, ** P < 0.01, *** P < 0.001. Normalized to *Gapdh*; Dunn's multiple comparisons test.

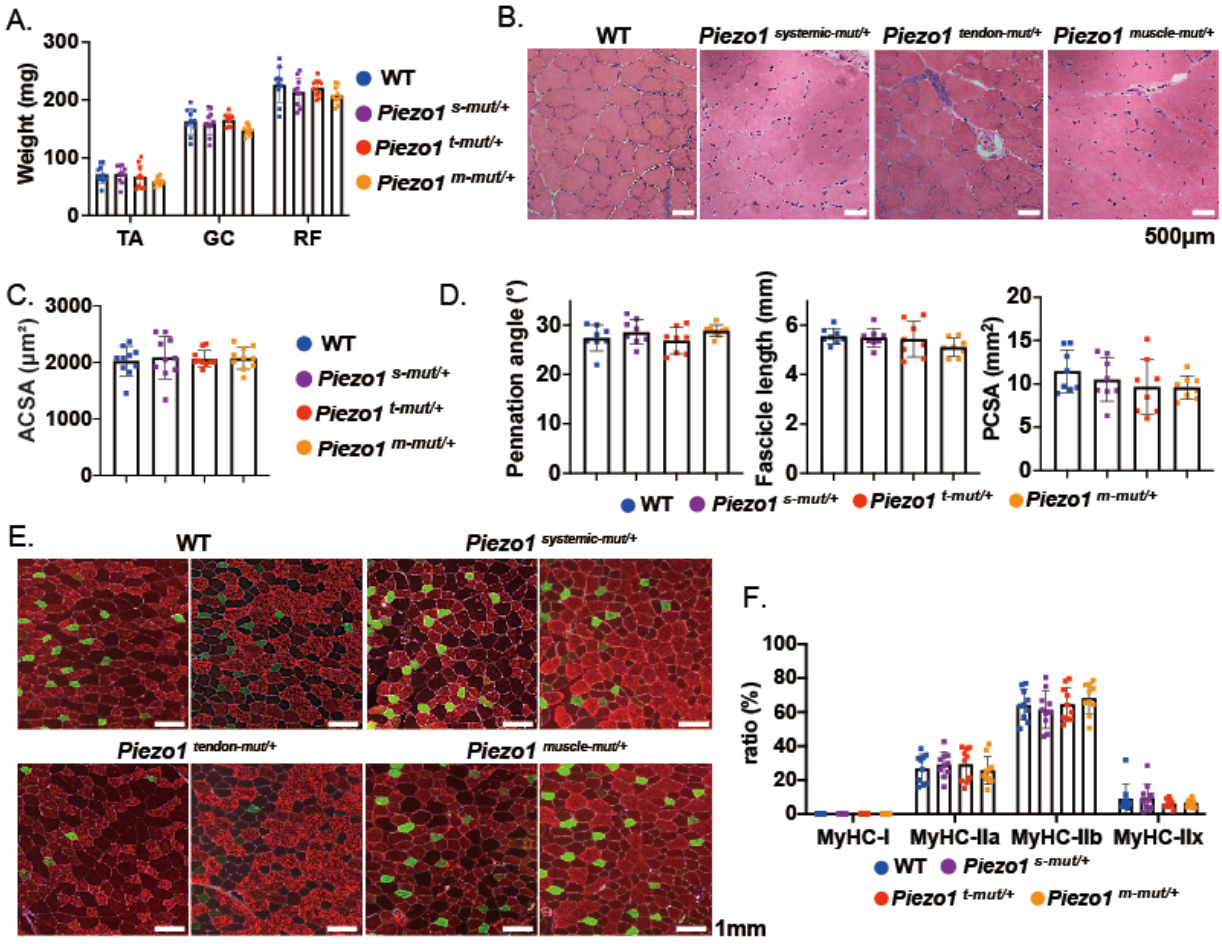

Fig. 4. Muscle tissue evaluation of tissue-specific R2482H *Piezo1* mice.
(**A**) Muscle weight of the tibia-anterior (TA), gastrocnemius (GC), and rectus femoris (RF) muscles of each mouse strain at 18 weeks of age. n = 10. Error bars represent SD, Tukey's multiple comparison test. (**B**) Representative images of H&E staining of the TA from each mouse strain at 18 weeks of age. Scale bars, 500 μm. (**C**) Anatomical muscle fiber cross-sectional area (ACSA) of the TA from each strain. n = 10. Error bars represent SD, and statistical differences were assessed using Tukey's multiple comparison test. (**D**) Pennation angle, fascicle fiber length, and physiological cross-sectional area (PCSA) of the TA muscle of each mouse strain at 18 weeks of age. n = 8. Error bars represent SD, Tukey's multiple comparison test. (**E**) Representative images of the TA immunohistochemistry of each strain. Scale bars, 1 mm. Purple: laminin; green: MyHC type 2x; red (left): MyHC type 2a; red (right): MyHC type 2b. (**F**) Positive ratio of each MyHC in the TA of each strain. n = 10. Error bars represent SD, Dunn's multiple comparison test.

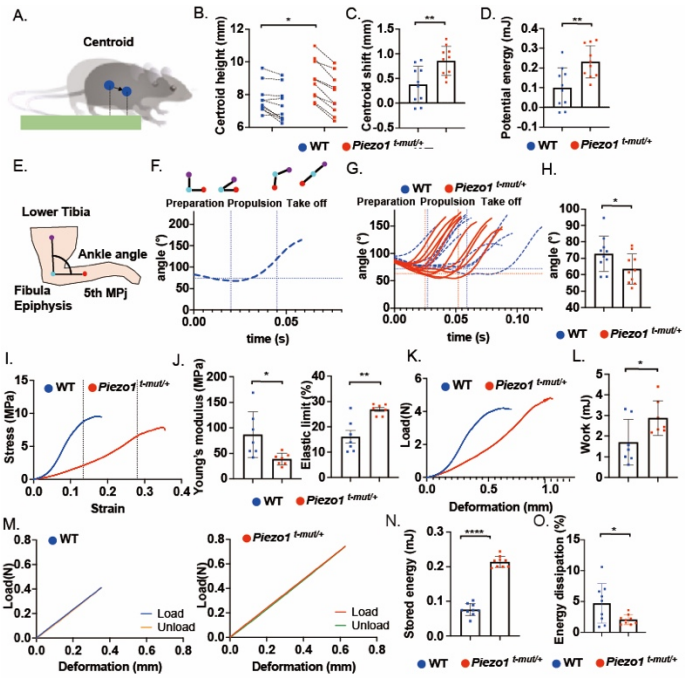

Fig. 5: Biomechanical properties of the R2482H *Piezo1* tendon.

(**A**) Schema of measuring centroid shift. (**B**) Centroid height at the start of the jumping motion and at the lowest point in WT mice and *Piezo1* $^{t\text{-}mut/+}$mice. n = 10. Error bars represent SD; * $P < 0.05$, ** $P < 0.01$; unpaired Student's t-test. (**C**) Centroid shift from the start of jumping motion to the lowest point in WT mice and *Piezo1* $^{t\text{-}mut/+}$mice. n = 10. Error bars represent SD, ** $P < 0.01$, unpaired Student's t-test. (**D**) Potential energy variation from the start of jumping motion to the lowest point in WT mice and *Piezo1* $^{t\text{-}mut/+}$mice. n = 10. Error bars represent SD, ** $P < 0.01$, unpaired Student's t-test. (**E**) Schema of ankle joint angle measurement (lower tibia-fibula epiphysis–5th metacarpal head angle). (**F**) Representative ankle joint angle motion of WT mouse. The phase of the jump is divided into three parts: preparation, propulsion, and takeoff. (**G**) All data of ankle joint angle motion in two genotypes. Blue dot curve lines: WT mice, red curve lines: *Piezo1* $^{t\text{-}mut/+}$ mice, longitudinal blue and red dotted lines: mean boundaries of the three phases in WT and *Piezo1* $^{t\text{-}mut/+}$ mice, respectively, transverse blue and red dotted line: minimum ankle angle degree in WT and *Piezo1* $^{t\text{-}mut/+}$ mice, respectively. (**H**) Angle at maximum flexion. n = 10. Error bars represent SD, * $P < 0.05$, unpaired Student's t-test. (**I**) Representative stress-strain curve for the mouse Achilles tendon. The displacement velocities were at constant speed of 0.05m/s. (**J**) Young's modulus and elastic limit of the Achilles tendon in WT mice and *Piezo1* $^{t\text{-}mut/+}$mice. n = 7. Error bars represent SD, * $P < 0.05$, ** $P < 0.01$, unpaired Student's t-test. (**K**) Representative load-deformation curve for the mouse Achilles tendon. The displacement velocities were at constant speed of 0.05m/s. (**L**) Work of the Achilles tendon in WT mice and *Piezo1* $^{t\text{-}mut/+}$mice. n = 7. Error bars represent SD, * $P < 0.05$, unpaired Student's t-test. (**M**) Representative hysteresis curve for the mouse Achilles tendon under conditions that mimic the preparation phase for each genotype. Blue and red lines: load curve; orange and green lines: unload curve. The displacement velocities mimicking jumping motion were 18.2Hz and 19.7Hz for WT mice and *Piezo1* $^{t\text{-}mut/+}$ mice, respectively. (**N**) Stored tendon energy in WT mice and *Piezo1* $^{t\text{-}mut/+}$mice. n = 9. Error bars represent SD, **** $P < 0.0001$, unpaired Student's t-test. (**O**) Energy dissipation ratios in WT mice and *Piezo1* $^{t\text{-}mut/+}$mice. n = 9. Error bars represent SD, * $P < 0.05$, unpaired Student's t-test.

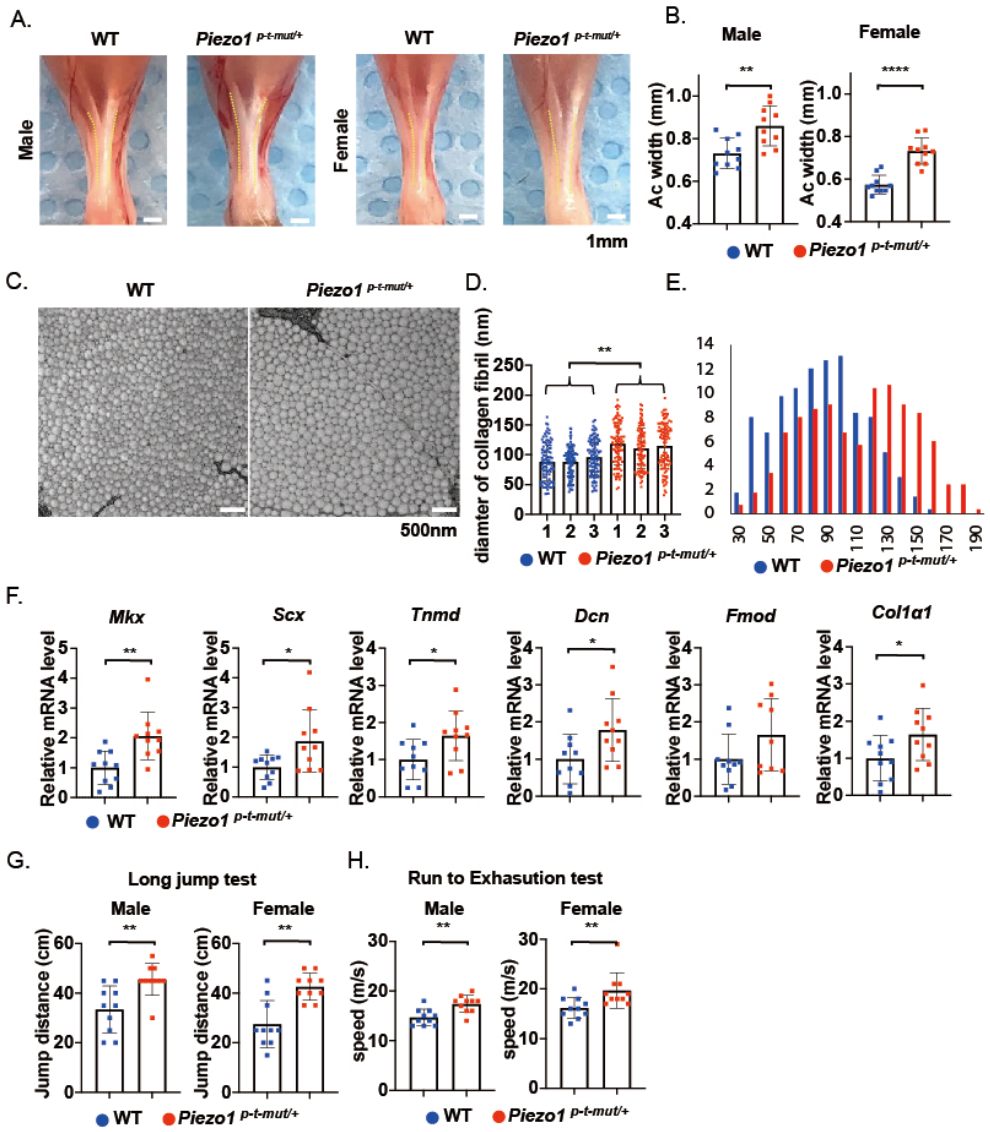

Fig. 6. Postnatal tendon-specific R2482H *Piezo1* enhances the physical ability along with tendon tissue enlargement.

(**A**) Representative images of the macroscopic views of the Achilles tendons of Scx-creERT2 (+) (= WT) mice and Scx-creERT2: *Piezo1* $^{cx/+}$ *(= Piezo1* $^{p\text{-}t\text{-}mut/+}$*)* mice 12 weeks after tamoxifen injection. Scale bars, 1 mm. (**B**) Width of the Achilles tendon of these mice. n = 10. Error bars represent SD; ** $P < 0.01$, **** $P < 0.0001$; unpaired Student's t-test. (**C**) Representative images of the transmission electron microscopy of the Achilles tendons of these mice. (**D**) The diameter of 100 collagen fibrils from these mice. n = 3 of each. For WT mice, mean diameter = 90.8 nm. For *Piezo1* $^{p\text{-}t\text{-}mut/+}$ mice, mean diameter = 140.8 nm. * $P < 0.05$, unpaired Student's t-test. (**E**) Histogram of the diameter of collagen fibrils. (**F**) qPCR analysis of the expression of the tendon-related genes in WT mice and *Piezo1* $^{p\text{-}t\text{-}mut/+}$ mice. n = 10. The mean mRNA values of these genes in WT mice were normalized to 1. Error bars represent SD, Normalized to Gapdh. * $P < 0.05$, ** $P < 0.01$; unpaired Student's t-test. (**G, H**) Maximum jump distance of each strain (G) and maximum speed of each strain (H). n = 10. Error bars represent SD, ** $P < 0.01$, Mann-Whitney test.

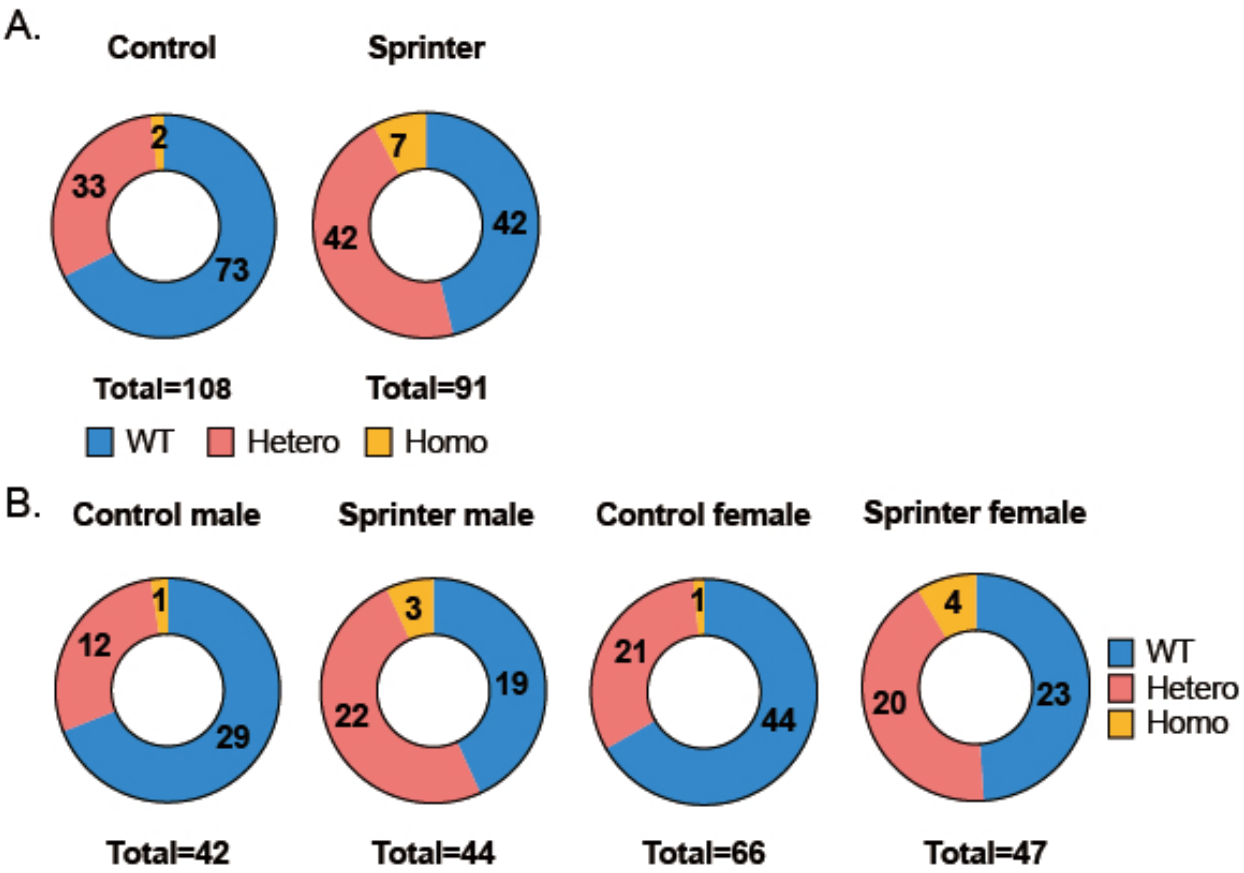

Fig. 7. Ratio of E756 deletion in Jamaican sprinters.
(**A**) Whole tables of E756del in Jamaican sprinters and controls. (**B**) Whole tables of E756 del in male and female Jamaican sprinters and controls.

All				
Genotype frequency				
Controls(%)	Athletes (%)	2 x 2 exact *P*	OR	95% CI
32.41	53.85	0.0026**	2.433	1.345 to 4.337
Allele frequency				
Controls(%)	Athletes (%)	2 x 2 exact *P*	OR	95% CI
17.13	30.77	0.0019**	2.15	1.323 to 3.496

Male				
Genotype frequency				
Controls(%)	Athletes (%)	2 x 2 exact *P*	OR	95% CI
30.95	56.82	0.0184*	2.935	1.219 to 6.961
Allele frequency				
Controls(%)	Athletes (%)	2 x 2 exact *P*	OR	95% CI
16.67	31.82	0.0223*	2.333	1.136 to 4.792

Female				
Genotype frequency				
Controls(%)	Athletes (%)	2 x 2 exact *P*	OR	95% CI
33.33	51.06	0.0803	2.087	0.9797 to 4.600
Allele frequency				
Controls(%)	Athletes (%)	2 x 2 exact *P*	OR	95% CI
17.42	29.79	0.0284*	2.011	1.084 to 3.826

Table 1. Genotype and Allele frequency of E756 deletion in Jamaican sprinters.
E756del frequency of Jamaican sprinters and controls, * $P < 0.05$, ** $P < 0.01$; 2 × 2 Fisher's exact tests and odds ratios.